Fivefold Twinned Nanoparticles

H. Hofmeister

Max Planck Institute of Microstructure Physics, D-06120 Halle, Germany

CONTENTS

- 1. Introduction
- Materials Synthesis and Formation Mechanisms
- 3. Stability and Phase Transitions
- 4. Structural Characterization
- 5. Properties and Applications
- 6. Summary

Glossary

Acknowledgments

References

1. INTRODUCTION

Twinning is widespread in crystalline materials of various origin and nature. Basic concepts and definitions of twinning are treated in many textbooks and review papers [1-3]. A description of the crystallographic fundamentals of twinning can be found in the International Tables for Crystallography, Volume D: "Physical Properties of Crystals" [4]. Twins may form as a result of erroneously attaching atoms or molecules to a growing crystal such that two crystals appear to be growing out of or into each other. Character and rule of twinning can be understood by considering the sequence of atomic layers added to a crystal during growth. Stacking of closepacked planes in face-centered cubic crystals is possible in three different positions denoted A, B, and C leading to a regular growth sequence ABCABCABCA. If, for example, the central A layer of this sequence is followed by a layer of misplaced atoms assuming the wrong position C, upon which a regular stacking appears again, then the following sequence will form: ABCABCACBACBA. In this way the crystal lattice is mirrored at the central layer A, which is easier to see if the central letter A is replaced by a vertical line | representing a mirror or twin plane: ABCABC|CBACBA. There are two general types of twin style: contact and penetration [5, 6]. The one considered here is contact twins that have a composition plane, the twin plane, that forms a boundary between the twinned subunits.

Twinning often has a serious effect on the outward shape and symmetry of a crystal, in particular in the case of repeated twinning. Two types of repeated twinning are known: lamellar and cyclic. Lamellar twinning forms from parallel contact twins repeating continuously, one after another. Cyclic twinning requires nonparallel coplanar composition planes. If these twin planes enclose an angle being an integer part of 360°, then a complete circle can be formed by cyclic twinning. Some classic minerals like cassiterite (SnO₂), wurtzite (ZnS), and rutile (TiO₂) form cyclic twins called "trilling," "fourling," "sixling," or "eightling" quite according to their twin angles of 120°, 90°, 60°, or 45°, respectively. Cyclic twinning is also found in minerals of the spinel (MgAl₂O₄) group whose specific rule of twinning bears its name, the spinel twin law. Here a twin plane is parallel to one of the octahedral habit planes enclosing an angle of 70.53°, which is close to $2\pi/5$. Repeated cyclic twinning according to this twin law does not form a complete circle, but leaves a small gap. Nevertheless, it enables the formation of "fivelings" of a number of crystals.

Actually, repeated twinning, also called polysynthetic twinning, or multiple twinning, is rather common in natural minerals and crystalline materials. There are also known examples of twin compounds composed of cyclicly arranged twin pairs [7]. However, it is the type of fivefold twinning on alternate coplanar twin planes in small particles, creating "fivelings" of unique morphology, for which the term "multiply twinned particles" (usually abbreviated as MTPs) was applied. The term MTP will herewith be used for such particles, otherwise, for example, for fivefold twinning in thin films, the term "fivefold twinned structures" is used. The unique morphology of MTPs and the unusual symmetry of the arrangement of building units are essential structural features, mostly at dimensions of a few nanometers, but fairly often also up to micrometer or even millimeter dimensions.

Fivefold twinning in thin films and nanoparticles of nanometer dimensions is in itself a whole class of materials, the origin of widespread structures resulting from a great variety of substances and fabrication processes involved. These are introduced in this chapter together with the issues of synthesis, formation mechanisms, and stability and lattice defects. Various illustrative examples are aimed at emphasizing the importance of this phenomenon in the area of nanostructured materials. It always has attracted the attention not only of crystal growth and crystallography research,

but also of cluster physics, physical chemistry, surface science, thin film growth, and materials research. The occurrence of quintuples of twins and local fivefold structures includes also quite different materials systems ranging from biological materials to minerals, such as proteins [8], polyoxometalates [9], viruses [10], surfactant bilayers [11], natural diamond [12], and self-assembled metal nanoparticle superlattices [13]. Within the minerals, even particular diamond species of extraterrestrial origin, which were contained in meteorites, are found [14]. Appropriate examples will be mentioned when discussing various aspects of fivefold twinning. This chapter is accompanied by an almost complete list of references that makes available results and experiences of previous work in a greater context.

1.1. Crystallographic Characteristics

The characteristics of materials that favor MTP formation are: (i) face-centered cubic (fcc) or diamond cubic (dc) crystals, (ii) low twin boundary energy, and (iii) a surface energy anisotropy with, for example, $\sigma\{111\} < \sigma\{100\}$, where {111} and {100} are the indices of surfaces of lowest energy for cubic crystals. However, any other crystal allowing repeated cyclic twinning with twin angles of about $2\pi/5$ would fit as well, if the twin boundary energy is not exceedingly large. The structural peculiarities of such particles comprise the following characteristics: (i) They are composed of equisized subunits of tetrahedral shape, (ii) the subunits join together on adjacent bounding faces (twin planes), (iii) the subunits enclose an angle of $\sim 2\pi/5$, and (iv) the involved tetrahedra share common axes of fivefold symmetry. Shape and composition of particles formed according to the above construction scheme are (i) the decahedron (pentagonal bipyramid), consisting of 5 tetrahedra with 1 fivefold axis, bounded by 10 triangular faces, and (ii) the icosahedron, consisting of 20 tetrahedra that share 6 fivefold axes and one common point at the center, bounded by 20 triangular faces. Composition and shape of the decahedron (point group symmetry D_{5h}) and the icosahedron (point group symmetry I_h) are schematically shown in Figure 1. As tetrahedral subunits of regular fcc or dc lattice, respectively, cannot form a complete space-filling structure, there remains an angular misfit (resulting in a gap of 7.35° for the decahedron), which is not considered in the drawings. Strictly speaking, the fivefold axes in such materials are only of pseudo-fivefold symmetry, unless there is some rearrangement of the lattice.

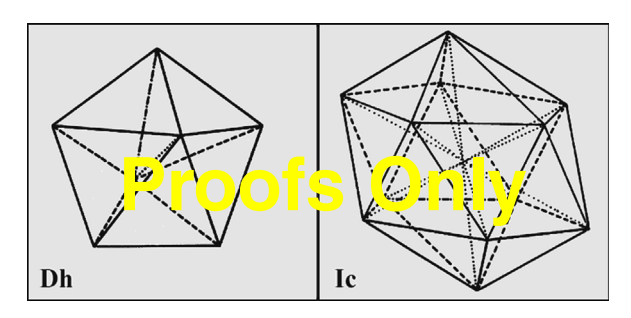


Figure 1. Shape of MTPs and their composition of tetrahedra: (Dh) decahedron and (Ic) icosahedron. Adapted with permission from [220], H. Hofmeister, *Cryst. Res. Technol.* 33, 3 (1998). © 1998, Wiley-VCH.

For single crystalline particles of most of the materials (cubic crystals) considered here, the common growth form is that of a cuboctahedron that is bounded by triangular octahedron faces, or {111}, and square cube faces, or {100}. This semiregular or Archimedian solid is drawn as a hard sphere model in Figure 2. Different from that, MTPs such as the icosahedron (Platonic solid), also drawn in Figure 2, are bounded by triangular faces of equal type, or {111}, only. This octahedron face is energetically favored for fcc and dc crystals because of the surface energy anisotropy of most of these materials, as in according to the above mentioned condition (iii) of MTP formation. That is how MTPs minimize their surface energy by approaching a spherical shape, which is most effectively achieved with the icosahedron.

1.2. Modes of Appearance

The mode of appearance of fivefold twinned particles depends on both their orientation with respect to a planar substrate (or a matrix) and the evolution of their surface morphology as influenced by the growth conditions. With respect to a planar substrate, there are four possible high symmetry orientations for both types of MTPs. Decahedra may be situated (i) with their fivefold axis perpendicular to the substrate plane, as in "fivefold" orientation or (011); (ii) with the fivefold axis parallel to the substrate plane, as in "parallel" or (001); (iii) with one tetrahedral bounding face resting on the substrate, as in "face" orientation or (111); and (iv) with the common edge of two tetrahedra resting on the substrate, as in "edge" orientation or (112). As can be seen from Figure 3, this gives as projection on the substrate (or imaging) plane a regular pentagon, a rhombic, a shortened pentagon, or a slightly less shortened pentagon, respectively. Icosahedra may be situated (i) with the common edge of two tetrahedra resting on the substrate and two fivefold axes parallel to it, as in "edge" orientation or (112); (ii) with one corner resting on the substrate and one fivefold axis parallel to it, as in "parallel" orientation or (001); (iii) with one fivefold axis perpendicular to the substrate, as in "fivefold" orientation, or (011); and (iv) with one tetrahedral bounding face resting on the substrate, as in "face" orientation or (111). Figure 4 shows the corresponding projections on the imaging plane giving a hexagon shortened along a diagonal, a hexagon elongated along a diagonal, a regular decagon, or a regular hexagon, respectively. The assignment of orientations in terms of crystal axes indices (in braces)

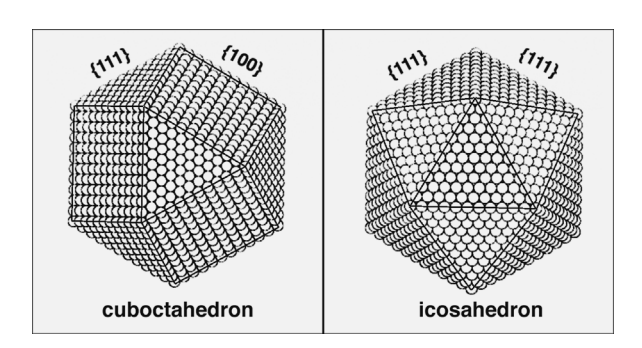


Figure 2. Hard sphere models of the surface morphology of cuboctahedron and icosahedron.

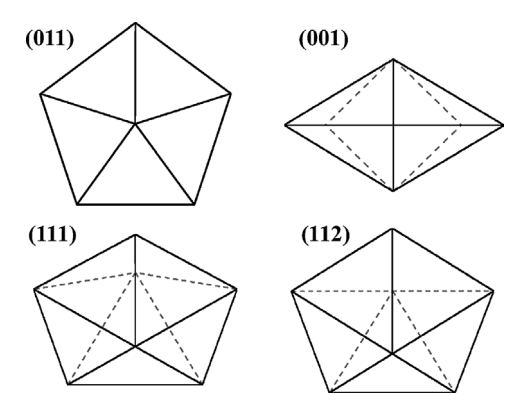


Figure 3. Orientation of decahedra on a substrate: "fivefold" (011), "parallel" (001), "face" (111), and "edge" (112).

concerns one, two, or five tetrahedra situated in the corresponding orientation.

The growth conditions are usually described by a growth parameter α that relates the rates of growth along different crystal directions. For fcc or dc materials, it is given by $\alpha = \sqrt{3v_{100}/v_{111}}$, where v_{100} is the growth velocity of cube faces and v_{111} is that of octahedron faces. The effect of α on the crystal morphology is a continuous variation starting, for example, with a perfect cube shape for $\alpha = 1$, via the cuboctahedron shape shown in Figure 2 for $\alpha = 1.5$, which corresponds to thermal equilibrium growth, to the octahedron shape for $\alpha = 3$. Under thermal equilibrium, the growth morphology may also be described by a parameter β relating the surface free energies ε_{100} and ε_{111} of the lowest energy surfaces. However, crystal growth usually is far from thermal equilibrium; thus the shape evolution is not characterized by minimizing the surface energy, but rather the growth rate of each face as determined by the kinetics. For MTPs this may lead to deviations from the ideal shapes introduced above, which range, for example, for the decahedron from a star-shaped (A) to a strongly faceted (B) and a prism-shaped specimen (C) corresponding to a variation of growth parameters from 3 to 2 and 1.5, respectively, as shown in Figure 5. Shapes B and C are named

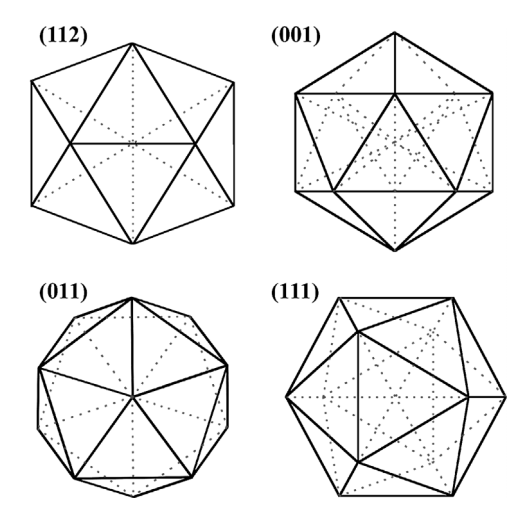


Figure 4. Orientation of icosahedra on a substrate: "edge" (112), "parallel" (001), "fivefold" (011), and "face" (111).

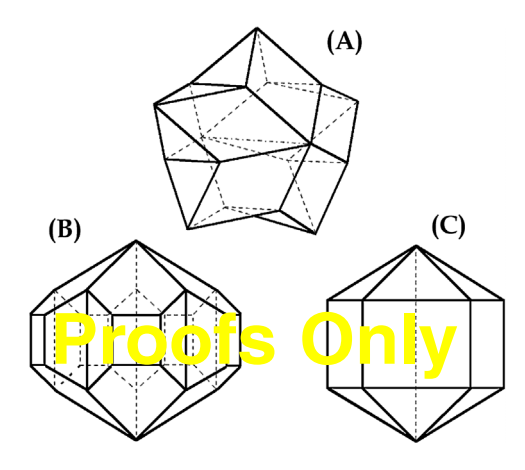


Figure 5. Deviations from the ideal shape of decahedra: (A) star-shaped, (B) faceted (Marks), and (C) prism-shaped (Ino).

"Marks decahedron" [15, 16] and "Ino decahedron" [17] by those who first introduced the corresponding models. An example of the formation of re-entrant edges, where twin boundaries emerge to the surface, as well as faceted dimples at the emergence points of fivefold axes, represents the Cu decahedron in Figure 6. Accordingly, re-entrant edges, faceted dimples, and pyramidal capping of triangular faces may occur at icosahedra [18].

1.3. Features of Fivefold Twinning

1.3.1. Natural Origin

Fivefold twinning, being a widespread habit of nanoparticles and nanostructured materials, actually is not only found in synthetic materials, but also in structures with a natural origin. As a most striking example, one may mention the polyhedral forms of certain viruses and their pentagonal aggregation. This was predicted in 1956 by Crick and Watson [19] and was confirmed in 1958 and later, mainly by electron microscopy means [10, 20–23]. Another example from biology is the hollow icosahedron configuration *in vivo* of

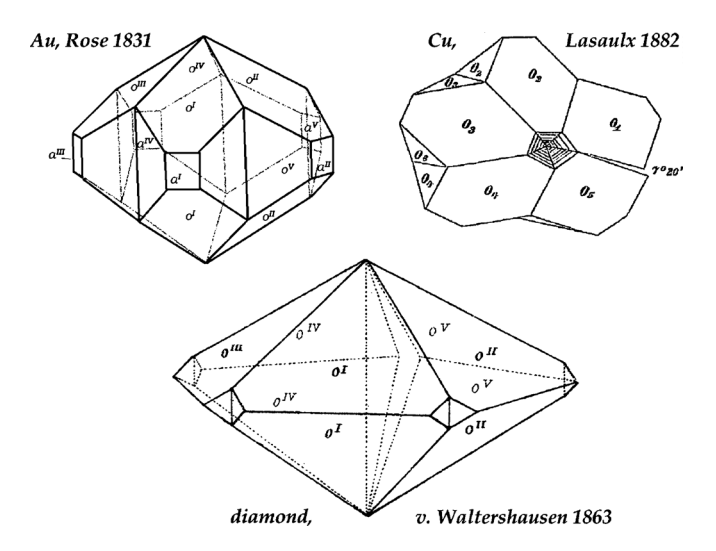


Figure 6. Early findings of fivefold twinning (fivelings) of natural occurrence.

certain protein supermolecules [8]. In the course of studying the presolar history of matter, fivefold twinned diamonds of extraterrestrial origin have been found in meteorites [14, 24]. By far, the most numerous and earliest examples of natural occurrence of fivefold twinning are known from the field of mineralogy. In former centuries, an essential part of the contemporary materials science was developed by mineralogists, mining engineers, and metallurgists. Thus it is understandable that in the first half of the 19th century the natural formation of "fivelings" in some minerals was known and therefore reported subsequently in textbooks and shape catalogues [25–29].

It was as early as 1831 that Rose [30] reported the observation of a strongly faceted decahedron of gold, the schematic drawing of which, shown in Figure 6, is an astonishing precursor of the Marks decahedron given in Figure 5B. Next to gold, fivefold twinning was also frequently observed in diamond of natural origin. This was reported for the first time by von Waltershausen [31]. Besides slightly faceting at the twin boundary tips, the original drawing, shown in Figure 6, contains a gap between subunits o^{IV} and o^V , corresponding to a defect caused by the lack in space filling with five tetrahedra. The first finding of a copper fiveling was reported 1882 by von Lasaulx [32]. This multiply twinned crystallite, also shown in Figure 6, is characterized by a nearly star-like shape and pentagonal dimples at the emergence of the fivefold axis. The indication of a $7^{\circ}20'$ gap between subunits O_1 and O_5 is based on theoretical considerations rather than on experimental observation. The MTPs of natural origin usually exhibit sizes around 1 to 2 mm. Further findings of natural fivefold twinned crystallites including, besides the already mentioned Au, diamond, and Cu, also Ag, sphalerite (ZnS), marcasite (FeS₂), magnetite (Fe₃O₄), and spinel (MgAl₂O₄), are presented together with the year of first mention of the corresponding mineral and related references in Table 1. One particular observation was reported by von Rath in 1877 [33] concerning an approximately 2 mm long pentagonal needle of gold whose shape corresponds to an elongated form of the prism-shaped decahedron in Figure 5C. This way, all essential shape variations of decahedra as introduced in Figure 5 were known by the end of the 19th century. The formation of fivefold twin junctions by cyclic twinning in naturally occurring substances, as confirmed by continued observations in the first half of the 20th century, was supported from a theoretical crystallography point of view by Herrmann [34]

Table 1. Natural occurrence of fivefold twinned structures.

Matter	(First mention) Refs.		
Au	(1831) [26, 28, 30, 33, 397, 398, 418]423]		
Ag	(1944) [29]		
Cu	(1882) [29, 32]		
C (dc)	(1863) [7, 12, 14, 24, 25, 27, 29, 31, 424, 425]		
ZnS	(1882) [7, 27, 32]		
FeS ₂	(1977) [426]		
$MgAl_2O_4$	(1877) [427]		
Fe_3O_4	(1984) [428]		
virus	(1958) [10, 20–23]		
protein	(1997) [8]		

who introduced the noncrystallographic point-groups D_{5h} of the decahedron and I_h of the icosahedron. A description of simple forms of these noncrystallographic classes was given by Niggli [35].

1.3.2. Synthetic Origin

The investigation of fivefold twinned structures in synthetic nanoparticles and thin films started in the second half of the 20th century by Segall [36] with the observation of pentagonal grains of pyramidal shape in cold rolled Cu upon thermal etching in 1957. This was followed in 1959 by the observation of pentagonal whiskers (i.e., rod-like shape) of Ni, Fe, and Pt grown from the vapor phase on W substrates by Melmed and Hayward [37] who also explained the peculiar shape by assuming five twinned fcc subunits with only slight lattice distortions. Mackay [38] presented in 1962 a hard sphere model of icosahedra, described them as being made up of 20 tetrahedra, discussed their characteristics, calculated the density of closed shell icosahedra, and demonstrated a mechanism of transition to the fcc structure. In the same year Schlötterer [39-41] reported on fivefold twinned pyramidal grains of Ni grown by electrodeposition, and one year later Wentorf [42] described fivefold twinned crystallites of synthetic diamond with indications of a small-angle grain boundary accommodating the angular misfit. In 1964 Faust and John [43] reported on Si and Ge fivefold twinned grains grown from the melt. Skillman and Berry [44] found fivefold twinned particles of AgBr grown from solution. Ogburn et al. [45, 46] communicated the observation of pentagonal dendrites of Cu grown from the vapor phase. Schwoebel [47, 48] reported pentagonal pyramids of Au grown in fivefold orientation on Au(110) and Au(100) surfaces, and Gedwill et al. [49] obtained fivefold twinned grains of pyramidal shape in the deposition of Co by hydrogen reduction of CoBr2, respectively. Similarly, in 1965 De Blois [50, 51] found the formation of pentagonal shaped whiskers of Ni by hydrogen reduction of NiBr₂. In the same year Bagley [52-54] proposed a model of pentagonal decahedra made up of five twinned tetrahedra whose orthorhombic lattice only slightly deviates from the fcc crystal lattice. In 1966 Downs and Braun [55] found fivefold twinned grains in the plating of Ni by thermal decomposition of nickel carbonyl.

The discovery of decahedral and icosahedral particles of Au and Ag formed in the early stage of thin film growth on alkali halide and mica substrates as well as by evaporation in inert-gas atmosphere in 1966 [56-64] is connected with extended availability and improved capabilities of electron microscopes at this time, which favored focusing on fivefold twinned structures of nanometer dimensions. This way, already in the first ten years of exploration, broad experimental evidence of the phenomenon, correct nomenclature, clear models, and reasonable insight in formation mechanisms was achieved. Since then a continuous and even increasing interest in fivefold twinned structures in nanoparticles and thin films produced a more than linear increase (from 1 in 1957 to 25 in 2001) of publications per year and was more and more devoted to technologically important materials like diamond, semiconductors, and Ni. The fivefold twin structure could be made visible, in particular, by

HREM as it is shown in Figure 7 by the example of a decahedron of Rh [65]. The HREM image (left) of the MTP situated in fivefold orientation (twin boundaries marked by =i.e.= arrow heads), as_in with the fivefold twin junction perpendicular to the image plane, together with the corresponding diffractogram (right) give a clear representation of its symmetry as well as spacings (e.g., of {111} and {200} planes) and angular relations of the lattice of the tetrahedral subunits involved. Utilization of dedicated experimental techniques like cluster source equipped molecular beam devices for synthesis [66] and real-time video recording equipped electron microscopes for characterization [67-71] enabled elucidating new models and mechanisms of MTP formation as well as uncovering a rich variety of new materials having such structures. The appeal of fivefold symmetry was tremendously encouraged with the disclosure of icosahedral quasicrystals and related phases [72-75] and with the invention of the quasilattice concept to describe these structures basing on local icosahedral packing of atoms contained in tetrahedrally close-packed and related phases of intermetallic compounds [76–79]. Between both fields there are certain relations from a structural point of view, such as via decagonal twinned crystalline approximant phases [79-82].

2. MATERIALS SYNTHESIS AND FORMATION MECHANISMS

2.1. Materials Overview

Fivefold twinned structures may be found in any crystalline material that allows twinning on alternate coplanar twin planes enclosing an angle of about $2\pi/5$. Favorite materials throughout the periodic table of elements are the transition metals Fe, Co, Ni, Cu, Ru, Rh, Pd, Ag, Ir, Pt, Au; the lanthanide's Sm and Yb; as well as the group II element Mg, group III elements Al and In, and group IV element Pb, that have fcc crystal lattice, at least for the modification present in multiply twinned particles. Additionally, the group IV elements C, Si, and Ge with dc crystal lattice contribute to the MTPs. Further, multiply twinned structures are known from a number of alloys like Au-(Fe, Co, Ni, Cu, Pd), Al-(Li, Cr, Mn, Fe, Cu, Zr), Ni-(Zr, Ti), Pt-(Fe, Rh), and Si-Ge. There exists also a considerable list of binary and ternary compounds from which MTPs have been reported, including AgBr; the nitrides and carbides BN, TiN, TiCN and

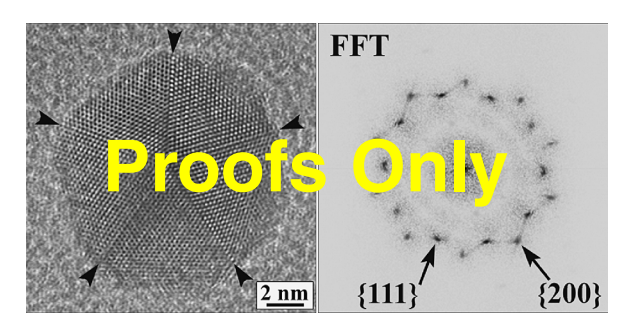


Figure 7. Decahedral particle of Rh in 5-fold orientation grown by vapor deposition on NaCl. Adapted with permission from [97], H. Hofmeister, *Mater. Sci. Forum* 312–314, 325 (1999). © 1999, Trans. Tech. Publications.

BC, Cr_2C_{2-x} , SiC; the oxides Fe_2O_3 , Fe_3O_4 , SnO_2 , $BaTiO_3$, and B_6O ; and further the compound semiconductors GaP, $CuInSe_2$, CdSe, and CdTe. The list of materials, to which even the molecular crystals fullerite C(60) and C(76) must be added, as well as supramolecular polyoxometalates and surfactants, is still increasing.

A summary of these materials together with their main characteristics and the routes of synthesis applied is given in Table 2, where elements, alloys, compounds, and composite materials with fivefold twinned structures are listed. For each entry, the table contains the year of first mention, the total number of publications known until now, and a number of representative references. This summary must be completed by composite materials consisting of MTPs embedded in a matrix like Ge, Si, or Si-Ge precipitates in Al alloys [83–88]; Cu precipitates in Ni-Zn-Cu alloy [89]; and Au, Ag, or Co precipitates in polymer or glass matrix [90–96]. As an example of matrix-embedded MTPs, Figure 8 shows a decahedral particle of Ag grown by precipitation in glass [97]. The HREM image (left) of the particle (twin boundaries marked by short lines) clearly shows its nearly spherical shape determined by the metal-matrix interface energy. The accompanying diffractogram (right) reveals symmetry, lattice plane spacings, and angular relations according to the approximately fivefold orientation. Another class of materials should be finally mentioned, namely colloidal crystals or self-assembled superlattices consisting of two- or threedimensional arrangements of metal nanoparticles that form fivefold twinned structures quite according to those previously described [13].

2.2. Routes of Synthesis

2.2.1. Vapor Phase Techniques

The synthesis of fivefold twinned nanoparticles and thin films may be proceeded by a large number of various processes and specific techniques. Generally, they differ by the state of the material applied in the synthesis. We distinguish synthesis (i) from the vapor phase, (ii) from the liquid phase, and (iii) from the solid phase. Vapor phase synthesis (i) includes (a) heterogeneous nucleation and growth of particles and thin films by various methods of either physical or chemical vapor deposition on substrates, and (b) homogeneous nucleation and growth of particles by aggregation within an inert-gas atmosphere. Most of the early work on metal MTPs has been done according to the process scheme given in (a) by thermal evaporation of the metal within an evacuated chamber and condensation of the metal vapor on appropriate substrates [57, 60, 98-111]. Physical vapor deposition was also applied in the formation of multiply twinned nanoparticles and thin films of Ge [112-121], SnO₂ [122], Fe_2O_3 [123], and C(60) or C(76) [124–128]. Chemical vapor deposition has been used for formation of multiply twinned nanoparticles and thin films, for example, of diamond [18, 129-132] (particles) and [133-146] (thin films), or Si and Si-Ge [147-149], TiN [150-152], TiCN [153, 154], SiC [152], GaP [155], and BN [74, 132] from precursor molecules, the decomposition or reaction of which provides the species deposited. The inert-gas aggregation technique (b) was successful in producing MTPs of most of the metals [64, 101, 156-167] and Si and Ge [168, 169], as well as alloys of

Table 2. Materials with fivefold twinned structures: (A) elements, (B) alloys, (C) compounds, and (D) composites.

	Synthesis	Characteristics	Refs.
A. Elements			
Mg (1981)	inert-gas aggregation, cluster beam expansion	decahedra, closed shell icosahedra	[160, 242]
Fe (1959)	PVD, inert-gas aggregation	decahedral whiskers, decahedra	[37, 101, 158, 159, 293]
Co (1964)	solid-phase reduction, inert-gas aggregation	decahedra, icosahedra	[49, 64, 293, =125] 430]
Ni (1959)	PVD, electrodeposition, inert-gas aggregation, colloidal synthesis	hollow whiskers, icosahedra, decahedra, thin films, rod-shaped decahedra	[37, 39, 157, 159, 165, 190, 200, 202, 204, 206, 208, 426] 431
Cu (1957)	electrodeposition, inert-gas aggregation, colloidal synthesis, PVD, e-beam	thin films, rod-shaped decahedra, icosahedra	[36, 39, 45, 98, 100, 157, 159, 178, 193, 231, 363, 388]
Ru (1988)	colloidal synthesis	structural fluctuations	[71]
Rh (1981)	solid phase reduction, PVD, colloidal synthesis, electrodeposition	decahedra, icosahedra	[65, 108, 226, 371, 374, 410, 435, 436]
Pd (1966)	PVD, inert-gas aggregation, electrodeposition, colloidal synthesis	decahedra, icosahedra, double icosahedra	[56, 63, 64, 99, 101, 107, 159, 161, 174, 198, 249, 438, 439]
Ag (1966)	PVD, inert-gas aggregation, electrodeposition, colloidal synthesis, e-beam	decahedra, icosahedra, rod-shaped decahedra	[60, 63, 98, 105, 157–159, 166, 174, 205, 207, 211, 217, 230, 255, 258, 291, 292, 349, 354, 44 0 , 441]
Ir (1997)	electrodeposition	decahedra, icosahedra, shape variations	[210, 216]
Pt (1959)	PVD, inert-gas aggregation, colloidal synthesis, electrodeposition	decahedral whiskers, shape variations, decahedra, icosahedra	[37, 104, 161, 191, 210, 376, 411, 444]
Au (1964)	PVD, inert-gas aggregation, colloidal synthesis, electrodeposition, solid-phase reduction	decahedra, icosahedra, rod-shaped decahedra, double icosahedra; self-assembled nanoparticles superlattice	[13, 40, 47, 57–59, 61, 62, 64, 105, 106, 157–159, 161, 173, 182, 189, 210, 212, 237, 239, 240, 254, 259, 324–327, 335, 365, 366a, 378, 382, 387, 400, 407, 411, 447–450]
Sm (1992)	inert-gas aggregation	decahedra	[66]
Yb (1993)	inert-gas aggregation	decahedra, icosahedra	[162, 452]
Al (1997)	e-beam irradiation	decahedra, icosahedra	[232]
In (1999)	physical vapor deposition	decahedra, tetragonal lattice sub-units	[109, 111, 340]
C (dc) (1963)	high-pressure melt synthesis, CVD, dynamic-shock synthesis	decahedra, misfit faults, icosahedra, thin films, star-shaped & rod-shaped decahedra	[18, 42, 129–132, 138, 139, 141–143, 145, 350–352, 456, 457]
Si (1964)	melt growth, matrix precipitation, CVD, PVD, inert-gas aggregation	decahedra, misfit faults, thin films, star-shaped decahedra	[43, 147, 149, 168, 169, 185, 186, 234, 266, 270]
Ge (1964)	melt growth, matrix precipitation, PVD, inert-gas aggregation, solid phase crystallization, ion implantation	star-shaped & rod-shaped decahedra, thin films, decahedra	[43, 96, 112–116, 120]
Pb (2000)	inert-gas aggregation, PVD	decahedra, tetragonal lattice sub-units	[110, 164]
B. Alloys			
Au-Fe (1999)	PVD, electrodeposition	decahedra, icosahedra	[213, 385]
Au-Co (2002)	electrodeposition	decahedra, icosahedra	[213]
Au-Ni (2002)	electrodeposition	decahedra, icosahedra	[213]
Au-Cu* (1997)	inert-gas aggregation, electrodeposition	decahedra, icosahedra, rod-shaped decahedra	[170, 210, 215, 432]
Au-Pd (1990)	colloidal synthesis	decahedra of rounded shape	[428]
Fe-Pt (2002)	colloidal synthesis, inert-gas aggregation	decahedra, icosahedra, ordered phase transition	[171, 434]

Table 2. continued

	Synthesis	Characteristics	Refs.
Ni-Zr (1985)	rapid solidification	thin films, quasicrystal approximants	[80, 437]
Ni-Ti (1986)	rapid solidification	thin films, quasicrystal approximants	[437]
Rh-Pt (1990)	colloidal synthesis	decahedra	[371, 433]
Al-Li* (1985)	matrix precipitation,	thin films, icosahedra,	[219, 442, 443]
, ,	rapid solidification	quasicrystal approximants	
Al-Cr* (1993)	rapid solidification	star-shaped decahedra	[82, 187]
Al-Mn* (1985)	rapid solidification	thin films, icosahedra, star-shaped decahedra	[81, 82, 339, 451]
Al-Fe* (1987)	rapid solidification	thin films, quasicrystal approximants	[79, 188]
Al-Cu* (1988)	rapid solidification	thin films, icosahedra, quasicrystal approximants	[187, 442]
Al-Zr* (1985)	rapid solidification	thin films, tetrahedrally closed-packed structure	[453]
steel (1983)	steel processing	decahedra, tetrahedrally closed-packed structure	[454, 455] 2
Si-Ge (2001)	CVD	decahedra, thin films	[149]
C (60) (1992)	PVD, aerosol synthesis	decahedra, icosahedral clusters, star-shaped	[124–126, 128, 405]
C (76) (1995)	PVD	decahedra decagonal twinning	[127]
C. Compounds			
AgBr (1964)	solution growth	decahedra	[44, 429]
BN (1985)	CVD, e-beam irradiation	decahedra, thin films, star-shaped decahedra	[132, 228, 403]
TiN (1988)	CVD	rod-shaped & star-shaped decahedra, thin films	[150–152]
TiCN (1985)	CVD	decahedra	[153, 154]
BC (2002)	arc evaporation	icosahedra	[167]
Cr_3C_{2-x} (1991)	reactive sputtering	decagonal twinning	[183]
SiC (1996)	CVD	star-shaped decahedra	[152]
Fe_2O_3 (1983)	PVD	decahedra	[123]
SnO ₂ (1996)	PVD	thin films, multiple twin junctions	[122]
B ₆ O (1998)	high-pressure melt synthesis, pulsed laser deposition	icosahedra, hierarchic structure, decahedra	[179, 180, 184, 241, 341, 343]
BaTiO ₃ (1998)	solid phase chemical reaction	thin films, multiple twin junctions	[445, 446]
GaP (1988)	CVD	thin films, multiple twin junctions	[155]
CdTe (1993)	PVD	hollow whiskers	[406]
CuInSe ₂ (1994)	molecular beam epitaxy	thin films, multiple twin junctions	[353]
CdSe (2002)	colloidal synthesis	icosahedra	[418]
polyoxometalate	self-assembly	icosahedra, hierarchic	[9]
(2001) surfactant	self-assembly	structure hollow icosahedra	[11]
(2001)	,		. 1
D. Composites			
Co/polymer (2000)	colloidal synthesis	polytetrahedral packing	[93]
Cu/Ni-Zn-Cu (1993)	matrix precipitation	decahedra	[89]
Ag/glass (1991)	ion exchange, ion implantation	decahedra, icosahedra	[90, 94]
Au/polymer (1998)	colloidal synthesis, PVD	decahedra, icosahedra	[91, 92]
Ge/Al (1986)	matrix precipitation	decahedra, rod-shaped decahedra	[83, 84, 85, 86]
Si/Al (2001)	matrix precipitation	decahedra	[88]
Si-Ge/Al (2001)	matrix precipitation	decahedra	[87]
Ge/silica (2001)	ion implantation, co-sputtering	decahedra	[95, 96]

Note: Entries in italics refer to tenfold twinning, asterisk signs indicate possible changes of order or stoichiometry in alloys.

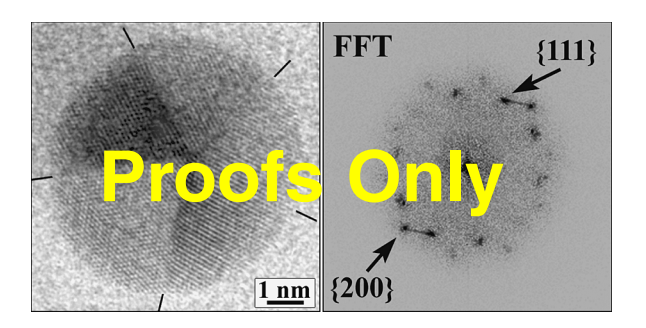


Figure 8. Decahedral particle of Ag in fivefold orientation grown by precipitation in glass. Adapted with permission from [97], H. Hofmeister, *Mater. Sci. Forum* 312–314, 325 (1999). © 1999, Trans. Tech. Publications.

Au-Cu and Fe-Pt [170, 171]. The process scheme given in (b) mainly enables particulate mass production of the corresponding material [159, 169, 172-174] and investigation of unsupported particles [164, 175–178]. The vapor phase route also includes modern techniques of materials synthesis such as pulsed laser deposition [179–181] and sputtering [95, 182, 183]. A typical example of growth from the vapor phase is given in Figure 9. The rhombic profile of the decahedral Rh particle [108] shown in the HREM image (left) is due to the (001) orientation of the base tetrahedral subunit relative to the electron beam. The accompanying diffractogram exhibits spots originating from {111}, {200}, and {220} lattice plane fringes of the (001) oriented base and two (112) oriented top tetrahedra marked by squares and circles, respectively. Additional spots marked by open arrows result from Moiré type contrast features in the particle center due to superposition of subunits of both orientations [166].

2.2.2. Liquid Phase Techniques

Liquid phase synthesis (ii) includes (a) growth from the melt and (b) growth from solution via precipitation by chemical means (b1) or by electrodeposition (b2). High-pressure melt growth was used for diamond [42] and B₆O [184] synthesis. Precipitation from alloy melt was utilized for the growth of Si and Ge MTPs [43, 185, 186]. Most of the quasicrystalline phases and their approximants have been produced by rapid cooling of Al-Mn and similar alloy melts [74, 187, 188]. The solution route (b1), or colloidal synthesis, has been frequently used for wet chemical formation of multiply twinned AgBr [44] and metal particles of Au, Ag, Cu, Pt,

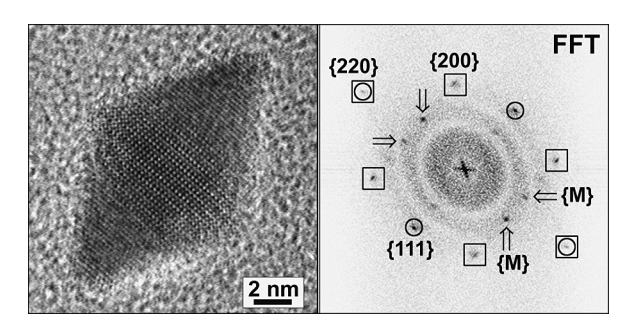


Figure 9. Decahedral particle of Rh in parallel orientation grown by vapor deposition on NaCl.

Pd, Ni, and Ru, as well as Pt- alloys [91, 189–198]. The solution route (b2), or electrodeposition, is widely utilized for fabricating protective coatings, mostly of Ni, whose appearance depends on grain size and texture, which may be controlled by the electrode potential. Fivefold twinned grains are the main constituents of films with (110) texture. Multiply twinned structures have been reported for Au, Ag, Cu, Pt, Pd, Ni, Ir, Rh, and Cu- alloys deposited as films [40, 199– 204] or particles [45, 205-213]. As it was mainly revealed by the work of Da-ling Lu [209, 210, 214-216], the crystal habit of fcc metal particles is controlled by the electrode potential in solution, as-in icosahedra and decahedra are formed at =i.e.= lower potential, whereas at higher potential less or no MTPs occur. Typical examples of MTPs grown from solution can be found in Figure 18 where HREM image contrast features of icosahedral Ag particles formed by hydrolysis of a mixed solution of tetraethoxy orthosilicate and silver nitrate in ethanol plus water [217] are presented.

2.2.3. Solid Phase Techniques

Solid phase synthesis (iii) includes several subroutes: (a) precipitation from solid solutions in crystalline or glassy hosts, (b) solid phase crystallization from the amorphous phase, (c) solid phase reduction by reactive gases like H₂ or CO of highly disperse metal compounds, and (d) irradiationassisted processing by electron beam or ion beam impact applied to induce particle formation in a matrix or on a substrate. Precipitation of fivefold twinned nanoparticles in crystalline matrix was reported for Au, Ag, Cu, Ni, Al-Li, Si, Ge, and Si-Ge [83-89, 181, 182, 186, 218, 219] where shape deviations, such as rod-like particle shapes, depending on orientation relations between precipitate and matrix as well as on the respective interface energy, were frequently observed. Precipitation of MTPs in glassy hosts was observed for Ag in soda lime glass, doped by ion exchange, upon thermal processing [90, 94, 220-222] and for Si in SiO_x by thermal decomposition of SiO [223]. Ag decahedra formed in glass matrix keep their structural peculiarities even when stretching the glass at elevated temperatures results in elongation of the previously spherical particles [220]. The amorphous-to-crystalline phase transition according to process scheme (b) has been studied intensively for thin films of Ge [113-117, 119, 224] and powder particles of Si [147, 148], which exhibit a distinct tendency to fivefold twinned structure formation. Solid phase reduction, or process scheme (c), has been used for decades to fabricate highly dispersed, supported metal particles, such as for application in heterogeneous catalysis. MTPs of Au, Ag, Cu, Rh, Co, and Ni are reported for this subroute [49, 50, 55, 217, 225-227] to occur on appropriate carriers. In recent years, a number of techniques for irradiation-assisted processing was developed to produce new nanoparticles and nanoparticulate composites. These techniques include electron beam irradiation to induce particle formation by reduction and aggregation of precursors where MTPs have been observed for BN, Ag, Cu, Al, Si, and Ge [95, 96, 228-234], as well as ion beam irradiation to introduce, as in to implant, =i.e.= dopants like Ag or Ge in a matrix so as to enable particle formation. MTPs originating from the latter technique were

found for Ag and Ge in glassy hosts [94-96]. Finally, as a

further route to fivefold twinned nanostructures, one should mention here the self-assembly of ligand-stabilized metal nanoparticles into superlattices of two or even three dimensions [13] that exhibit fivefold twin junctions similar to the pentagonal aggregations of virus particles [22]. When using a micelle route to preferentially create multiply twinned metal particles [235, 236], one could compose in this way a fivefold twinned superlattice of MTPs.

2.3. Formation Mechanisms

2.3.1. Nucleation-Based Formation

The formation of MTPs and fivefold twinned structures is an important issue, since understanding of the relevant mechanisms may help to control conditions for preferred formation or prevention of such structures. The great variety of materials and processes involved cannot be attributed to only one mechanism of formation. In general, we distinguish (i) nucleation-based and (ii) growth-mediated formation of fivefold twins. The nucleation (i), or noncrystallographic packing of atoms, is complemented by layer-by-layer growth in the course of which the noncrystallographic arrangements transform to quintuples of twins. The growth-mediated formation (ii) may proceed by cyclic twinning operations due to (a) misstacking of atoms (growth twinning) or (b) mismatch of lattices (deformation twinning) during growth.

MTPs are observed in the nucleation stage (a) of thin film growth on substrates via physical [237-240] and chemical vapor deposition [18, 129, 130], as well as in inert-gas aggregation [159, 161], melt growth [241], solution growth [189], electrodeposition [201], and solid phase crystallization [116]. Sometimes the noncrystallographic nature of the nuclei formed is emphasized by the name "paracrystalline nuclei" [201]. The preferred formation of closed shell structures with icosahedral arrangement is confirmed by the observation of magic numbers in the mass spectra of transition metal clusters [242-248]. Fcc metal clusters obey the building plan of Mackay icosahedra [38] as it has been shown for five-shell Pd clusters of 561 atoms by direct imaging [249]. The first steps of evolution for such clusters, starting from a 1 shell nucleus, by shape maintaining layerby-layer growth, contain 13, 55, 147, 309, 561, ... atoms as schematically drawn is shown in Figure 10. Likewise, pentagonal decahedra may evolve from a nucleus of decahedral shape whose initial growth sequence contains 7, 23, 54, 105, 181, ... atoms. During growth the noncrystallographic packing of atoms is transformed to a fivefold twinned arrangement of translationally ordered subunits whose small size enables compensation of the angular misfit [92].

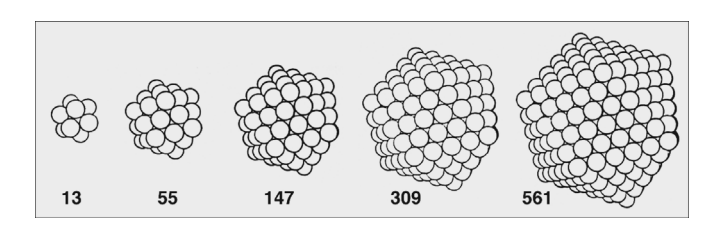


Figure 10. First steps of fcc closed shell cluster evolution of icosahedral shape.

The nucleation of fivefold symmetry in dc materials proceeds, according to their bonding characteristics, via cage rather than closed shell structures having pentagonal dodecahedron (20 atoms) and truncated pentagonal bipyramid (15 atoms) shapes, which are analogues of icosahedron and decahedron, respectively. The first steps of a layer-like growth sequence of decahedral shape, containing 15, 60, 140, 265, 490, ... atoms are illustrated in Figure 11. With the dodecahedron nucleus, a growth sequence of 20, 100, 292, 568, 994, ... is obtained when its 12 pentagonal faces are decorated by truncated pentagonal bipyramids. Always three of these attached cages of the first layer share one atom, at which formation of a tetrahedral subunit of a dc lattice may start in the course of further layer-like growth [250, 251]. In the above cluster models, the tetrahedral bond is preserved with bond angles and bond lengths only slightly differing from that of bulk dc crystals. The outer atoms have dangling bonds that may be saturated, for example, by hydrogen. 15 atoms and 20 atoms hydrogenated carbon cage clusters correspond to the hydrocarbon molecules hexacyclopentadecane and dodecahedrane [252], respectively, which are assumed to be effective in the nucleation of diamond MTPs by methane decomposition [129]. The formation of fivefold twinned structures of Ge was proposed to originate from a 15 atoms nucleus formed in the amorphous phase [116]. A 100 atoms cluster first has been proposed to explain defect structures in the heteroepitaxial growth of Si on spinel [250].

2.3.2. Growth-Mediated Formation

If not nucleated from the beginning, MTPs also may form during growth by repeated cyclic twinning. The main source of growth twinning is misstacking of atoms at faces of low growth rate so as to produce reentrant edge configurations, which enable accelerated growth along a twin boundary [43, 117, 120, 186, 253]. In the particle stage of growth, twinning may proceed by the formation of primary, secondary, and tertiary twins on pre-existing tetrahedra as shown schematically in Figure 12. This process is found to operate not only to form decahedra, but also icosahedra by successive stacking of tetrahedra. Rather soon after the nucleation mechanism has been introduced, alternatively the tetrahedra stacking mechanism began to be discussed [57, 93, 169, 205, 254–257]. First it was been observed during in situ investigation of the epitaxial growth of Au on MgO [258] and was later confirmed by an ex situ study on the growth of Au on

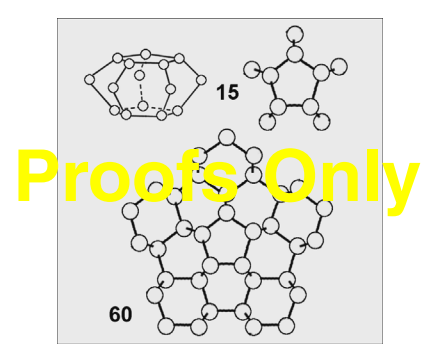


Figure 11. First steps of dc cluster evolution of decahedral shape.

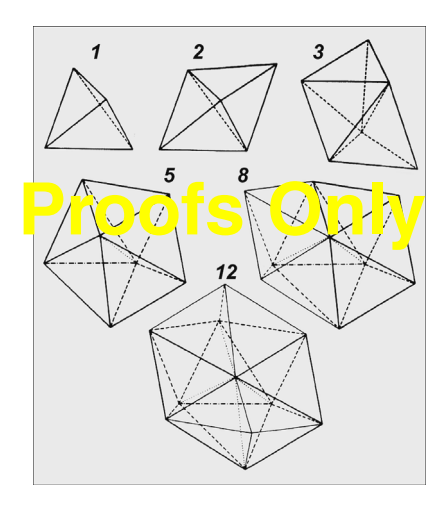


Figure 12. Successive stacking of tetrahedra in twin position resulting in MTP formation.

AgBr [259]. The formation of multiply twinned structures by successive twinning on alternate cozonal twin planes also has been found in thin film growth of Ni, Ge, and SnO₂ [117, 122, 134, 202, 260]. In all cases, the formation of triple twin junctions is a decisive step in favor of fivefold twinning. Frequently, networks of interlinked threefold and fivefold twin junctions are observed in these films. Local fivefold twinned structures have been considered as essential growth stimulating constituents of preferred fcc growth of van der Waals crystals [261–263].

In addition to misstacking of atoms during growth as one possible origin of repeated twinning, the intersection of stacking faults and twin lamellae, introduced into the lat-

tice of growing thin films because of plane strain deformations, must be considered. Deformation twinning may serve

as a means of relaxing plane strains. The ability of fivefold twinned structures to accommodate large interfacial strains due to lattice misfit and thermal expansivity differences is known from the heteroepitaxial growth of semiconductors on insulating substrates [155, 264-266]. Strain-induced twin formation starts with the introduction of 90° Shockley partial dislocations passing through the strained lattice [267–270]. Successive penetration of a strained lattice by dislocations on alternate twin planes consequently will lead to the cross-=i.e.=ing of twins. A simple case of twin intersection, as_in the penetration of a stacking fault SF through a twin T, observed in the solid phase crystallization of Ge thin films [117, 220], is shown in Figure 13. In the crossing region, a secondary twin is formed. At the intersection of stacking fault and twin boundary, five-membered rings occur resulting from dislocation reactions [270]. The latter will act as seeds of prospective fivefold twin junctions upon propagation of additional dislocations on adjacent planes and will also lead to an extension of the secondary twin.

Sometimes, the origin of a certain fivefold twinned structure cannot be attributed to only one of the above discussed formation mechanisms, but may result from an interplay of growth twinning and deformation twinning. At various stages of thin film growth, extended structures containing several individual multiple twins may occur. During thin film growth of Au and Ag, decahedral and icosahedral

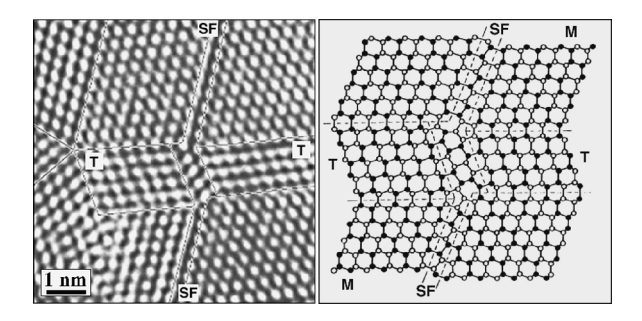


Figure 13. Secondary twin formation upon intersection of a twin band **T** by a stacking fault **SF** during solid phase crystallization of Ge. Adapted with permission from [97], H. Hofmeister, *Mater. Sci.* Forum 312–314, 325 (1999). © 1999, Trans. Tech. Publication.

MTPs have been observed to form polyparticles via coalescence preserving almost completely their previous structures [271, 272]. Networks of interlinked fivefold and threefold twin junctions have been found in electrodeposited Ni films having (110) texture [202, 204, 260]. Similar networks occur at advanced stages of the solid phase crystallization of amorphous Ge [114, 119, 120, 224, 253, 273] as well as in the chemical vapor deposition of diamond [134, 136, 139] and Si [149]. In the applied range of temperature and film thickness, it is generally assumed that kinetic factors dominate the growth that has been described as "solid-like growth" by Marks [272]. However, the formation of MTPs has also been discussed as being due to transformation to a higher symmetrical arrangement [274].

3. STABILITY AND PHASE TRANSITIONS

3.1. Stability of Fivefold Twins

Frequently, MTPs and fivefold twinned structures do not exist separately, but in coexistence or even competition with structures that exhibit regular crystal lattice without twins. Their stability is an intriguing issue mainly because of the discrepancy between noncrystallographic packing of atoms and its extension in three-dimensional space. Experimental and theoretical investigations of clusters, a few atoms up to several hundreds or even a few thousands of atoms in size, aimed at determining stable forms and their size limits, have been mostly done on rare-gas [262, 275-281] and transition metal [243, 246, 282-289] clusters produced in supersonic beams during gas expansion. Atomistic studies, using data from electron diffraction [164, 176–178, 276–278, 290–292] and mass spectrometry [242-244, 293, 294], by means of molecular dynamics and Monte Carlo simulations employing various pair interaction potentials [245, 247, 279, 280, 287, 295-297], revealed a wealth of knowledge on magic numbers and growth sequences [242, 244-248], thermal stability, shape and structure [246, 282, 284, 296, 298-307], phase transitions [248, 262, 289, 297, 308-316], and melting behavior [288, 310, 317] of clusters of icosahedral, decahedral, fcc crystalline, or disordered structure. However, there has been predicted not a global minimum of potential energy for a multitude of structural motifs and cluster configurations, but very small energy differences such that clusters do not necessarily have a single stable structure at realistic temperatures [282, 309, 317, 318]. Moreover, there has been found not a single sequence of phase transitions like icosahedral to decahedral to single crystalline fcc and its dependence on size and temperature, but also a reversal of this sequence [311] as well as a gradual instead of immediate transition [297, 308]. In addition, from molecular dynamics simulations there has been predicted, besides the layer-by-layer growth, also a certain probability of misstacking of atoms leading to island growth in twin position, which enables transition of decahedral to icosahedral shape by growth as it was experimentally observed on a much larger size scale [259]. Finally, experimental magic numbers associated with structures based on Mackay icosahedra have been classified by atomistic simulation to be of kinetic origin [319]. Even if the intermolecular potential disfavors the icosahedral structure, it occurs frequently due to potential characteristics that enhance kinetic trapping effects. The existence of such kinetic effects suggests that it will be possible to control structures of clusters and nanoparticles by tuning external parameters to enable design of nanomaterials properties.

The above findings are analogous to the configurational instabilities inherent to particles of sizes smaller than 8 nm [320, 321]. Real-time video recording of HREM investigations on very small metal particles revealed fast changes between a number of structures including cuboctahedra (single crystal), single twinned cuboctahedra, fivefold twinned decahedra, and icosahedra [67-71, 89, 322-327]. Some of these structures may be understood as result of a fivefold twin junction (also described as wedge disclination [328] or line disclination [329]) entering into and moving through a particle [330, 331]. Steps of this movement will include also asymmetric decahedra like the one of Ag shown as example in Figure 14. An eccentric position of the fivefold twin junction can be observed more often the smaller the particles are. The structural transformations observed along with a much higher rate of particle rotations in the presence of an electron beam may be understood in terms of statistical fluctuations with the probability of a particular configuration depending on size and temperature [320, 321].

MTPs consisting of regular fcc or dc subunits contain spatial discontinuities that introduce inhomogeneous strains. Additional strain and twin energy resulting from the specific composition of MTPs may be balanced by a reduction of surface energy up to a certain size above which trans-

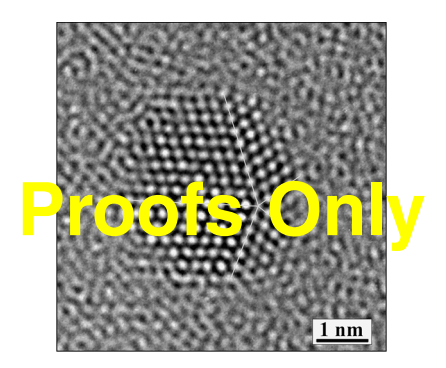


Figure 14. Asymmetric decahedral MTP of Ag grown by physical vapor deposition on alumina with eccentric position of the fivefold junction.

formation to single crystalline particles of cuboctahedral shape was expected. Strain relief by structural modifications such as homogeneous lattice distortions or the introduction of lattice defects as inhomogeneous lattice distortions may extend the range of stability. Energy balance considerations including cohesive, surface, adhesive (i.e., concerning particle/substrate interaction), elastic strain, and twin boundary energy aimed at calculation of stable size regions for MTPs of transition metals in comparison to their single crystalline counterparts [16, 17, 332] provide stable and quasistable size limits around 30 and 300 nm for icosahedral and decahedral MTPs of Ag, respectively. Transitions from multiply twinned structures to single crystalline fcc have been observed for very small metal particles in gas expansion experiments by electron diffraction techniques from which crossover sizes of 3.8 nm have been derived for Cu [333], whereas in comparable experiments a size-independent transition was found for Ag [178] and a dependence on the type of inert gas was found for Pb [164]. On the other hand, experimental studies on MTPs gave evidence of their extension to sizes far above the size limits derived from stability considerations (see Section 4.1). One of the reasons for this behavior is =4.2.= that they may undergo lattice transformations and in many cases exhibit lattice defects.

3.2. Lattice Transformations and Defects

The lack in space filling that results when composing MTPs of regular fcc tetrahedral subunits raises the question of whether the lattice of some or all of these subunits may adopt a slightly changed state of uniform distortion. To allow for the absence of spatial discontinuities in MTPs, some kind of structural modification or lattice defect is needed. This may be brought about by elastic strains acting on the tetrahedral subunits as first described by S. Ino to calculate their stability [17]. A slight, uniform distortion, for example, transforms the tetrahedral subunit fcc lattice into one having body-centered orthorhombic (B€O) point group symmetry =bco= so as to enable a Bagley decahedron with twin angle 72° [52–54]. Figure 15 shows the fcc unit cell of lattice parameter a inside which a BCO unit cell of lattice parameters=bco= **a**, **b**, **c** is drawn. As long as $\mathbf{a} = \sqrt{2} \mathbf{b}$ and $\mathbf{b} = \mathbf{c}$ (i.e., the nearest neighbor distance), the inscribed tetrahedron has fcc characteristics. The required uniform distortion is achieved

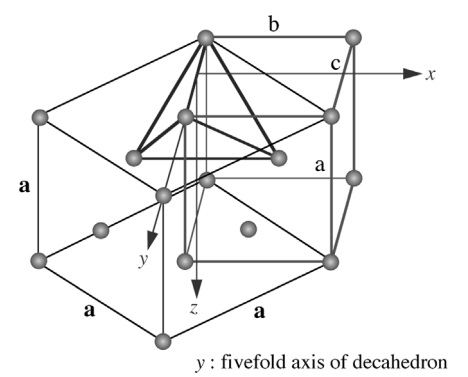


Figure 15. Tetrahedral twin subunit of a decahedron transformed from fcc to BCO lattice. =bco=

by applying a biaxial stress to elongate c (c = 1.0515 b) and to shorten a (a = 1.3764 b) [334]. This transformation preserves the close packing, but widens the angle between the triangular faces meeting at the y-axis from 70.52° to 72°. Another uniform distortion transforms the tetrahedral subunit fcc lattice into one having rhombohedral (rho) point group symmetry so as to enable a Mackay icosahedron with twin angle 72° [38]. Figure 16 shows the fcc unit cell of lattice parameter a inside which a rho unit cell of lattice parameters **b** is drawn. As long as the rhombohedral cell angle is $\alpha = 60^{\circ}$, the inscribed tetrahedron has fcc characteristics. By applying an uniaxial stress along the cube diagonal direction close packing is preserved in the icosahedron with a rhombohedral structure, but α is enhanced to 63.43° [334]. The nearest neighbor distance however is different now for interplane atoms ($\mathbf{b} = OA$, OB, OC) intraplane atoms ($\mathbf{c} =$ AB, AC, BC) with c = 1.0515 b. Consequences of these model considerations for lattice characteristics, diffraction patterns, and image contrast features have been demonstrated by crystallographic and electron microscopy studies on Au particles [334–338].

Accommodation of the angular misfit by transformation to the rho lattice has been reported also for Al-Mn multiple twins [339]. Contrary to the above examples where lattice distortions are assumed uniformly throughout all tetrahedral subunits, there are also reports about tetragonal lattice distortions in only one or two subunits while the remaining tetrahedra exhibit fcc lattice. This behavior has been observed for decahedral MTPs of In [109, 111, 340] and Pb [110]. The lattice of In bulk metal usually has base-centered =bct=tetragonal (B€T) point group symmetry and adopts fcc structure only in multiply twinned nanoparticles, whereas the lattice of Pb bulk metal usually has fcc point group =bct= symmetry and adopts B∈T structure not only in MTPs, but also in single crystalline and single twinned nanoparticles. Icosahedral MTPs of the Fe-Pt intermetallic phase have been assumed to adopt the L10 superstructure, which was not found in untwinned nanoparticles of this material [171]. Interestingly, the L1₀ superstructure has not only promising magnetic properties, but also enables formation of perfect decahedra without any need of distortion. Based on this structural characteristic, an icosahedron model has been proposed that consists of two such L1₀ decahedra, having

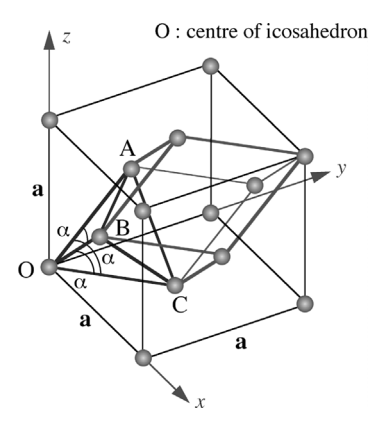


Figure 16. Tetrahedral twin subunit of an icosahedron transformed from fcc to rho lattice.

one common vertex and their fivefold axes in line, completed by a "belt" of ten slightly distorted tetrahedra [171]. It should be noted here that, similar to chemically ordered L1₀ decahedra of Fe-Pt, icosahedra of a few materials have been found that do not require elastic straining to close the angular gap, because their lattice characteristics already fit to the condition that the tetrahedron angle α amounts to 63.43°. This has been reported for MTPs of C(76) having monoclinic lattice [127], for B₆O where oxygen atoms are three-coordinated to icosahedral B(12) clusters in a rho lattice [179, 180, 184, 241, 341], as well as for BC with rho lattice [167]. Although clusters having fivefold symmetry are well known as entities in crystal structures [342–344], up to now only the above mentioned B(12) have been found to be arranged in hierarchical packing from which icosahedral MTPs may form.

Elastic strains in fivefold twinned structures of fcc and dc materials determine not only the general structural characteristics [16, 17, 275, 328, 332, 345, 346], but also that of the twin boundaries involved [347]. At sizes distinctly above 10 nm, inhomogeneous elastic strains [348] allow rather large reductions of the strain energy stored in MTPs such that stress relief processes may occur involving the formation of lattice defects [332]. Typically, planar defects such as stacking faults and secondary twin boundaries are observed [115, 321, 349]. A particular stress-relieving configuration observed in fivefold twinned structures of Si and Ge [115, 117, 169] is shown in Figure 17. It consists of regular arrays of tetrahedrally arranged stacking faults emerging at stairrod dislocations. Such stacking of fault arrays results in an angular lattice dilatation in the respective twin subunit, while the neighboring subunits remain undistorted. Two pairs of stacking faults are sufficient to accommodate the angular gap at the length scale of the particle shown here. More extended arrays in combination with small angle boundaries have been observed at Si particles of larger dimensions. Localized strains, defects, and misfit faults, which often simply consist of a small angle boundary, are by far the most reported inhomogeneities in MTPs and fivefold twinned structures of diamond [27, 129, 350-352], Si [169], TiN [151], and CuInSe₂ [353]. Individual dislocations

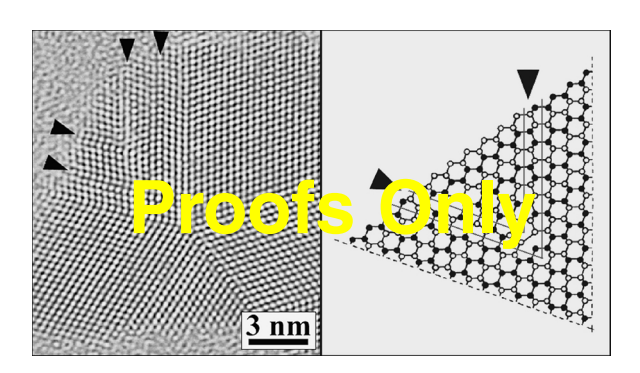


Figure 17. Array of two pairs of stacking faults (marked by arrow heads) emerging from stair- rod dislocations in one tetrahedral twin subunit of a Ge MTP (left) and the corresponding model representation of a twin sub-unit with one pair of stacking faults (right). Adapted with permission from [220], H. Hofmeister, *Cryst. Res. Technol.* 33, 3 (1998). © 1998, Wiley-VCH.

[105, 349, 354] and point defect agglomerations [107, 348] are rather scarcely observed.

Electron diffraction as employed to the study of cluster

4. STRUCTURAL CHARACTERIZATION

4.1. Characterization Methods

4.1.1. Electron Microscopy and Diffraction Methods

beams using refined methods of diffraction peak analysis [164, 176-178, 277, 278, 290-292], similar methods have =ed=been applied in XRD studies [305, 355], enabling one to distinguish between MTPs and single crystal structures on a scale of only a few nanometers or even less. The importance of electron microscopy for structural characterization of MTPs and fivefold twinned structures in synthetic materials from the very beginning has already been pointed out in 1.3.2. Section 4. This essential role results from the submicrometer size scale at which the phenomenon of multiple twinning mostly was found, thus being the actual domain of electron microscopy structural characterization. Utilization of a considerable number of methods and techniques ranging from simple shadow casting [10, 40] to state-of-the-art investigations devoted to, for example, observation under ultrahigh vacuum and at low temperature conditions [111], revealed many of structural characteristics that otherwise could not have been elucidated. Within the continuously increasing number and quality of electron microscopy studies, there have been employed electron diffraction pattern recording of individual MTPs and calculation of such patterns [337, 356–362], in situ experiments to follow growth and transformation processes inside the electron microscope [234, 255, 258, 355, 363], weak-beam dark-field and related imaging modes for visualizing the internal structure of MTPs [259, 335, 336, 364, 365], HREM [105, 109, 191, 217, 273, 325, 326, 349, 354, 366–373] and corresponding image contrast calculation [121, 174, 175, 347, 362, 369, 372, 374–391], tilt series to study how external shape and internal structure of MTPs change with their orientation to the electron beam [166, 190, 192, 362, 392], real time observation of fast processes such as structural fluctuations or particle coalescence [67, 70, 322, 323, 325, 326, 381, 393], and combination of XRD or X-ray absorption spectroscopy (EXAFS) investigations with TEM

4.1.2. Selected Area Electron Diffraction

or HREM studies [194, 355, 394].

Special attention is devoted to selected area electron diffraction (SAED), from which fivefold symmetry may be recognized in a direct manner, and HREM, from which unique "fingerprints" may be obtained. Actually, before and besides HREM imaging, it is the SAED pattern of an individual decahedron in fivefold orientation, one of the first was published 1964 by Schlötterer [40] and another striking example 1972 by Ino et al. [395], which is directly convincing and allows one to examine with high accuracy the symmetry as well as spacings and angular relationships of multiply twinned particles. To illustrate the capabilities of this method, Figure 18 shows as an example the SAED pattern of a decahedral Ni grain in fivefold orientation within an

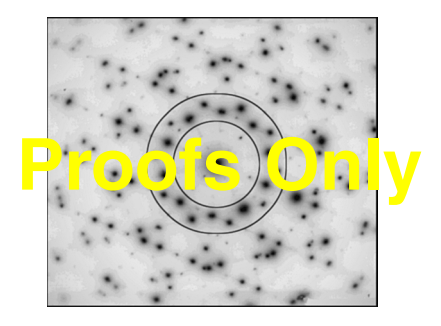


Figure 18. Selected area electron diffraction pattern of a decahedral Ni grain (fivefold orientation) within an electrodeposited thin film.

electrodeposited thin film having (110) texture. This grain of about 400 nm extension in a plane perpendicular to its fivefold axis exhibits secondary twin boundaries in two of the tetrahedral units. Accordingly, in the diffractogram a slight splitting of related spots of {111} and {222} type can be seen, which indicates an inhomogeneous relaxation of elastic strains due to the space filling gap. For the sake of clarity, no assignment of spots has been added to the SAED pattern, but two circles are drawn enclosing the innermost spots of {111} and {200} type. From this rather complex electron diffraction pattern, it can be clearly seen that not one single crystal, but a grain consisting of five subunits in well-defined orientation relationship are transmitted by the electron beam. Likewise, diffraction patterns from regions of 1 nm size of multiply twinned Au nanoparticles obtained by means of a microdiffraction equipment operated in the scanning transmission mode [396] confirm the particle composition of twinned subunits.

4.1.3. High Resolution Electron Microscopy

Imaging of lattice plane fringes by high resolution electron microscopy of MTPs frequently reveals, in combination with diffractogram analysis and image contrast calculation, a clear signature of particle shape and internal structure [166, 382, 384, 385, 390]. This is demonstrated in Figure 19 for Ag icosahedra arranged in various orientations with respect to the electron beam. It comprises HREM image, diffractogram, particle model, and diffractogram scheme of the particles in "face" orientation, "edge" orientation, "fivefold" orientation, and one tilted around 10° out of "edge" toward "fivefold" orientation (from top to bottom). The edge length of the HREM images corresponds to 4.8 nm. These image contrast features depend on the configuration of tetrahedral subunits that are oriented such as to give rise to lattice plane contrasts. In the "face" oriented icosahedron, for example, there are six twin planes parallel to the electron beam, or the axis of observation, leading to six sets of {111} lattice plane fringes. However, there must be considered superposition of lattice plane fringes where tetrahedral units are stacked one above another. That is why the image details cannot be straightforwardly interpreted in terms of lattice planes and increasingly become more complicated the more superposition occurs. The highly complex contrast patterns in HREM images of icosahedral particles due to superposition of various lattice segments cause corresponding complex spot patterns in the diffractogram. However, the frequently observed

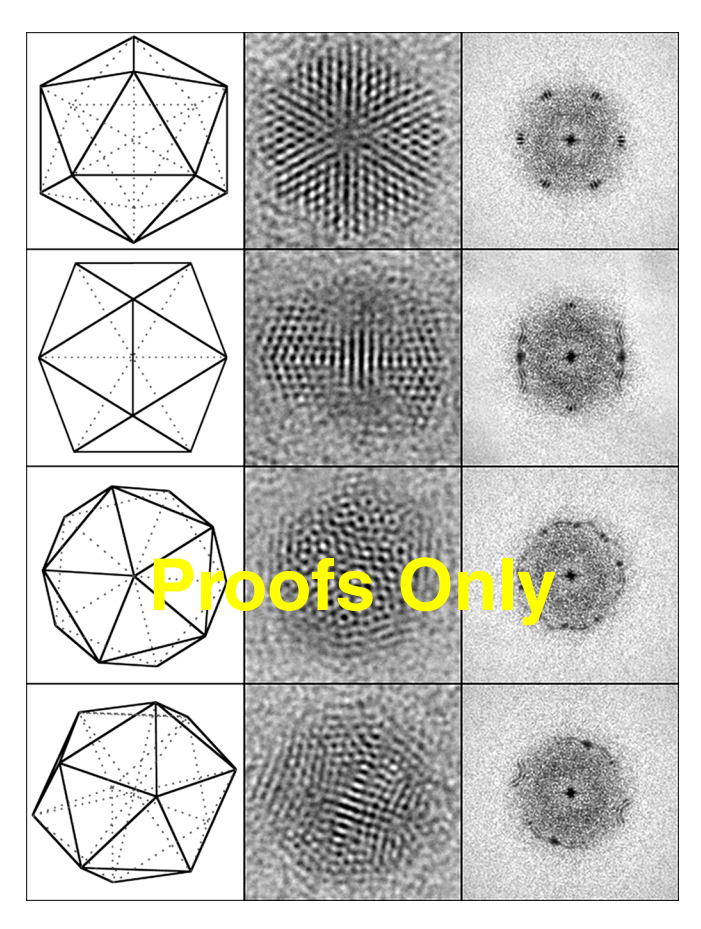


Figure 19. HREM "fingerprints" (edge length 4.8 nm) of icosahedral Ag particles in various orientations: "face," "edge," "fivefold," and tilted around 10° out of "edge" toward "fivefold," from top to bottom, together with diffractogram (right) and model (left).

diffractogram spot splitting, as shown in Figure 19, is no

direct evidence of angular misalignment or spatial mismatch of the lattice of twinned subunits. Actually, the shape of image regions of equal lattice plane fringe arrangement is =i.e.= reflected in the diffractogram fine structure [390], as=in, it is related in a certain way to the electron diffraction spot fine structure of polyhedral crystallites observed ear-[397] lier [396]. The fine structure of diffractogram spots also is found for calculated HREM images of icosahedra assuming a rho pointgroup symmetry without any lattice defects. By Fourier transform processing of various projections of tetrahedral subunit model images, the interference nature of the phenomenon has convincingly been demonstrated [390].

4.2. Size and Shape

The additional strain and twin energy associated with the formation of MTPs may be balanced by a reduction of sur3.1. face energy up to a certain size (see Section-8), above which transformation to single crystalline structures is expected. Experimentally observed fivefold twinned structures however, not only frequently exceed the size limits based on thermodynamic considerations, but also exhibit distinct deviations from the nearly spherical shape into various types of rod-like or even star-like particle shapes. One reason for

this behavior is the accommodation of angular misfit by the introduction of lattice transformations or lattice defects (see Section=9. Another reason is that obviously certain growth 3.2. conditions not only favor deviation from the ideal MTP shape (see Section 3), but also enable exceedingly large par-1.2. ticle size. Besides the two examples of Figures 20 and 21, which show a large decahedral MTP of Pd in "fivefold" orientation and a large icosahedral MTP in "parallel" orientation, the most impressive examples of extremely large MTPs of various materials (i.e., those having micrometer size and above) are compiled in Table 3. These include decahedral particles of the molecular C(60) crystal fullerite [125] exceeding the millimeter scale of size, and icosahedral particles of boron suboxide B_6O [341] with sizes around 40 μ m. While most of the MTPs on the micrometer scale are of decahedral shape, the above-mentioned extraordinary large icosahedra forming material exhibits a rhombohedral structure with a rhombohedral unit cell angle of $\alpha = 63.1^{\circ}$ being very close to the one for ideal icosahedral twinning.

Multiply twinned rod-like particles may form from decahedral nuclei by preferential growth along the fivefold axis. First observations were made within Au crystals of natural occurrence [33, 398-400]. Different from regular decahedra, these particles exhibit extended prism faces of {001} type. Their multiply twinned nature is revealed most easily from tilting experiments in the electron microscope, as has been shown recently for rod-like silver particles grown by inertgas evaporation technique [166]; this reference also sums up the literature about MTPs of rod-like shape in synthetic materials. As may be concluded from the model shown in Figure 5C, rotation around the long axis of the particle, situated perpendicular to the electron beam, is found to produce two characteristic image contrast patterns, separated from one another by 18° rotation, both having rotational periodicity of 36°. According to a rather recent publication, decahedral nanorods have also been fabricated via a bioreduction route [401]. Elongation of icosahedral MTPs toward rod-like shape may be achieved not simply by growth, but by successive growth twinning, this way reaching beyond the shape of complete icosahedra. As shown by the model in Figure 22, particles of elongated shape can be formed by stacking two icosahedra into each other such that they share five tetrahedra grouped around a common fivefold axis, as in a decahedron. Characteristic image contrasts of triple rhombic shape result from positioning one of the fivefold axes

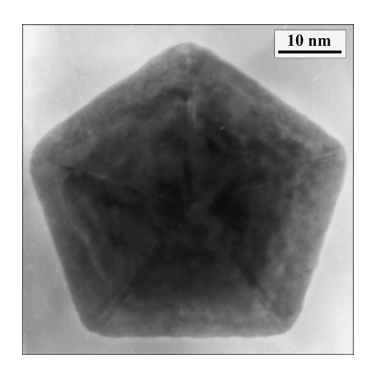


Figure 20. Decahedral particle of Pd in fivefold orientation grown on KI substrate by vapor deposition.

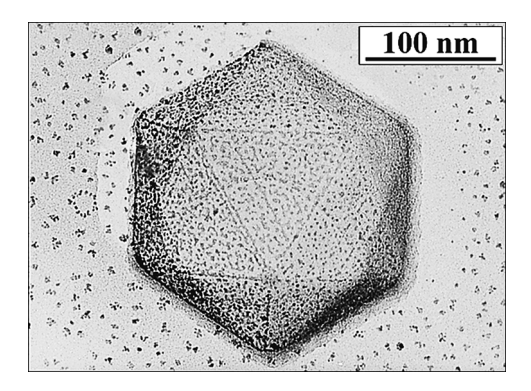


Figure 21. Pt-C shadow casting of an icosahedral particle of Ag grown on AgBr substrate by vapor deposition. Adapted with permission from [220], H. Hofmeister, *Cryst. Res. Technol.* 33, 3 (1998). © 1998, Wiley-VCH.

of these particles, being their long axis, parallel to the substrate, or perpendicular to the electron beam [387]. Hence the three decahedral regions involved show {111} lattice plane fringes within rhombic areas (shaded in Figure 22). In addition, these decahedra in "edge" orientation exhibit {220} lattice plane fringes within square areas (hatched in Figure 22). From atomic-scale simulations of copper polyhedral nanorods [391, 402], both types of rod-like MTPs have been found as stable geometrical structures. Multiply twinned particles of star-like shape may form, as deviation from the decahedron shape, by reduced growth rate along the five twin boundaries of the tetrahedral subunits. Hence,

Table 3. Size extrema found in fivefold twinned materials.

Material	Approx. size	Туре	(Year) Ref.
Cu	100 μm	Dh	(1957) [36]
diamond	$100 \mu m$	Dh	(1963) [42]
Ni	$3 \mu m$	Dh	(1964) [40a]
Si	$500 \mu m$	Dh	(1964) [43]
Co	$40 \mu m$	Dh	(1964) [49]
Ni	$8 \mu m$	Dh	(1966) [55]
Ni	\sim 2 mm	Dh (rod)	(1966) [51]
Ag	$100 \mu m$	Dh	(1968) [46]
Cu	$300 \mu m$	Dh	(1969) [225]
diamond	1 mm	Dh	(1972) [12]
(natural)			
Ni	$50 \mu m$	Dh	(1976) [207]
Au (natural)	$800 \mu m$	Dh (rod)	(1978) [398]
diamond	$600 \mu m$	Dh	(1979) [350]
TiN	5 μm	Dh (rod)	(1988) [150]
C (60)	2 mm	Dh	(1993) [125]
Yb	$1.5~\mu\mathrm{m}$	Dh	(1993) [162]
TiN	$10 \mu m$	Dh (star)	(1996) [152]
SiC	$50 \mu m$	Dh (star)	(1996) [152]
Au	$60 \mu m$	Dh	(1996) [399]
B_6O	$40 \mu m$	Ic	(1998) [341]
Au	$4~\mu\mathrm{m}$	Dh (star)	(2001) [212]
Si	$40 \mu m$	Dh (star)	(2001) [88]
Cu	$1 \mu m$	Dh (rod)	(2000) [392]
surfactant	$1~\mu \mathrm{m}$	Ic (hollow)	(2001) [11]
bilayer			
BC	$10 \mu m$	Ic	(2002) [167]
Pd	$1~\mu\mathrm{m}$	Dh, Ic	(2002) [198]

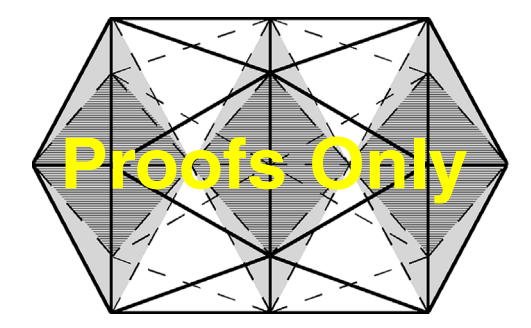


Figure 22. Schematic drawing of a "twinned icosahedron" particle consisting of 35 tetrahedral subunits.

these tetrahedra exhibit {111} truncations at their peripheral corners resulting in a star decagon projection when viewed in "fivefold" orientation. Star-like MTPs first have been reported for Cu of natural occurrence [32] and later for synthetic materials such as diamond [18, 42], Ge and Si [43, 88, 185], BN [132, 403], colloidal gold [212, 404], TiN and SiC [151, 152], Al-Cr-Si alloy [82], and also C(60) [405]. Finally it should be mentioned that a number of multiply twinned structures are hollow, as=in they exhibit an =i.e.= external shape of fivefold symmetry but an internal void of variable extension. Hollow fivefold twinned structures are mainly found in whiskers of pentagonal cross-section [50, 51, 406] and in organic materials such as proteins or surfactant bilayers [8, 11].

5. PROPERTIES AND APPLICATIONS

5.1. Structure-Sensitive Properties

Physical and chemical properties of materials assembled of fivefold twinned nanoparticles may differ from materials consisting of untwinned nanoparticles in a variety of aspects according to their respective structural characteristics. These differences concern properties sensitive to the surface energy, the lattice symmetry, the internal structure, and the surface structure, and they may cause changes, such as of the melting point, magnetic moment, electronic transition, and chemical reactivity, respectively. For MTPs embedded in a matrix of foreign material instead of the surface structure, the interface structure has to be considered, which via particle-matrix interaction may influence the elastic properties of the composite. In studies devoted to the properties of multiply twinned nanoparticles mostly the influence of their real structure on heterogeneous catalysis is stressed [65, 108, 156, 163, 217, 226, 363, 371, 374, 407-412] since adsorption and reactivity are highly structuresensitive properties. In a very recent investigation, Au MTPs have been found to lower selectivity and activity in the partial hydrogenation of unsaturated aldehydes with respect to the desired product allyl alcohol [227]. That means MTPs of Au are not useful for this reaction path. For separated Au(55) clusters of closed shell composition, an extraordinary high resistance against oxidation has recently been reported [413] that most probably is due to their icosahedral morphology. Tetrahedral subunits with the rho lattice of B₆O perfectly fit together at a common vertex without dislocations needed to accommodate an angular gap, thus enabling the

growth of rather large icosahedra of boron suboxide [179, 180, 184, 241, 341]. Consequently, glide planes are locked in these particles that may result in a low density material of extraordinary hardness. Quite similar is the situation with massive icosahedral crystals of boron carbide, for which the well known hardness of this compound could be further improved because of being multiply twinned with icosahedral symmetry [167]. Precipitation hardening in structural alloys of AL-Si-Ge is dependent on the precipitate morphology, which is largely determined by twinning [87]. Multiply twinning completely changes the interface with the matrix, and consequently the strengthening effect of these precipitates in the metal matrix is reduced. Since the formation of multiple twin junctions apparently promotes the growth of Si nanowires in the oxide-assisted route [414], it will be interesting to see to which extent this structure may influence the optoelectronic properties of the material.

5.2. Symmetry-Dependent Properties

The appearance of spontaneous ferromagnetic order in Pd nanoparticles of about 6.8 nm size has been explained by a transition from single crystalline to multiply twinned structure with decreasing size [313]. The icosahedral symmetry is considered to contribute to the onset of ferromagnetic ordering or to the increase of an already existing magnetic moment. The main driving force in this transition has been shown to be the strong surface anisotropy of fcc single crystals being replaced by the energetically more stable icosahedral arrangement below the above size [313]. Stoichiometric Fe-Pt nanoparticles of 3 to 6 nm in size are found to preferentially exhibit icosahedral structure upon appropriate thermal processing [171]. Icosahedral MTPs of this alloy are assumed to be stabilized by transition to the L1₀ ordered phase, which exhibits large magnetocrystalline anisotropy [171]. This may be the basis for future magnetic materials with nanometer dimensions. For studying their physical properties the Raman, Brillouin, and elastic tensors of materials that exhibit fivefold point group symmetry have been calculated [415–417]. Concerning the optoelectronic properties of nanoparticles there is a very recent report on an excellent combination of fluorescence spectroscopy and HREM of isolated semiconductor nanoparticles allowing both methods to be applied to the same specific particle [418]. This way changes not only in size, but also in **that** structural as well as morphological characteristics can be correlated to fluorescence properties of isolated nanoparticles. First results of the investigation of CdSe nanoparticles on transparent Si₃N₄ substrate indicate that the emission of strong fluorescence is not restricted to single crystalline particles of about 8 nm size, since icosahedral MTPs of slightly smaller size also show such emission [418]. More and systematic studies are needed to ascertain the role of the respective structural characteristic in this behavior.

6. SUMMARY

The aim of this chapter is to emphasize by illustrative examples and comprehensive references the importance of the widespread habit of fivefold twinning in nanostructured materials and to shed some light on the multitude of its facets. In particular, it shall enable us to link synthesis and processing of technologically promising or even important materials, their fivefold twinning characteristics, and their physical and chemical properties. This also includes the issue of comparing nanoparticulate materials, which preferentially have fivefold twinned structure to those being mainly in the untwinned state (see, e.g., [227]). For more detailed reading about this fascinating and rather complex phenomenon, some review articles concerning experimental as well as theoretical work in this field may be recommended. These are "Structure of Small Metallic Particles," by M. Gillet [419]; "Noble Metal Clusters" by R. Monot [420], "Comparison Between Icosahedral, Decahedral, and Crystalline Lennard–Jones Models Containing 500 to 6000 Atoms," by B. Raoult et al. [279]; "Phase Instabilities in Small Particles," by P. M. Ajayan and L. D. Marks [320]; "The Energetics and Structure of Nickel Clusters: Size Dependence," by C. L. Cleveland and U. Landman [284]; "Experimental Studies of Small Particle Structures," by L. D. Marks [421]; "Growth and Structure of Supported Metal Catalysts," by P. J. F. Harris [411]; "Preferred Structures in Small Particles," by N. Doraiswamy and L. D. Marks [321]; "Shells of Atoms," by T. P. Martin [294]; "Crystallography of Clusters," by J. Urban [384]; "Pentagonal Symmetry and Disclinations in Small Particles," by V. G. Gryaznov et al. [328]; and "Structure, Shape, and Stability of Nanometric Sized Particles" by M. J. Yacaman et al. [422]. The review "Forty Years Study of Fivefold Twinned Structures in Small Particles and Thin Films," by H. Hofmeister [220], gives a comprehensive record of four decades work (1957-1997) on fivefold twinned structures in small particles and thin films. The present chapter shall not only make available models and experimental findings of previous investigations in a greater context, but also stimulate future studies on this phenomenon.

GLOSSARY

Dislocation A line defect in a crystal, along which the lattice is displaced by a certain amount perpendicular or parallel to the dislocation line.

Ferromagnetic order Chemical order in a crystal that exhibits interaction at the atomic level, causing the unpaired electron spins to line up parallel with each other in a domain where a magnetic moment results.

Fluorescence The emission of light by a substance immediately after the absorption of energy from light of usually shorter wavelength.

Glide plane A low index crystal plane along which translation of one part of a crystal relative to the other part may proceed by the movement of dislocations.

Pair interaction potential Intermolecular potential describing the interaction between pairs of atoms derived from empirical models of interatomic bonding, used for computer simulation of bond energy and atomic structure of clusters.

Point group symmetry A method of denoting the combination of symmetry elements that a crystal contains.

Stacking fault A planar defect in a crystal where one part is displaced relative to the other part, such that the displacement does not correspond to a translational symmetry operation.

ACKNOWLEDGMENTS

This work is dedicated to Hans-Ude Nissen on the occasion of his 70th birthday. The author is greatly indebted to Christopher H. Gammons who drew his attention to the natural occurrence of gold fivelings that were known to mineralogists long ago. Special thanks are due to Wolfgang Neumann for many suggestions and critical discussions.

REFERENCES

- 1. R. Cahn, Adv. Phys. 3, 202 (1954).
- 2. P. Hartmann, Z. Kristallogr. 107, 225 (1956).
- I. Kostov and R. I. Kostov, in "Crystal Habits of Minerals" (M. Drinov, Ed.), p. 34. Academic Publishing House, Sofia, 1999.
- T. Hahn and H. Klapper, in "International Tables for Crystallography, D: Physical Properties of Crystals" (A. Authier, Ed.), <u>p. xxx.</u> Kluwer, Dordrecht, 2002. 2003.
- 5. M. L. Senechal, N. Jb. Miner. Mh. 518 (1976).
- 6. M. Senechal, Sov. Phys. Crystallogr. 25, 520 (1980).
- 7. C. Palache, Amer. Mineral. 17, 360 (1932).
- J. Walz, T. Tamura, N. Tamura, R. Grimm, W. Baumeister, and A. J. Koster, Mol. Cells 1, 59 (1997).
- A. Müller, P. Körgerler, and A. W. M. Dress, Coord. Chem. Rev. 222, 193 (2001).
- 10. R. C. Williams and K. Smith, Biophysica Acta 28, 464 (1958).
- M. Dubois, B. Demé, T. Gulik-Krzywicki, J.-C. Dedieu, C. Vautrin,
 S. Désert, E. Perez, and T. Zemb, *Nature* 411, 672 (2001).
- R. Casanova, B. Simon, and G. Turgo, Amer. Mineral. 57, 1871 (1972).
- 13. Z. L. Wang, Adv. Mater. 10, 1 (1998).
- 14. T. L. Daulton, D. D. Eisenhour, T. J. Bernatowicz, R. S. Lewis, and P. R. Buseck, Geochim. Cosmochim. Acta 60, 4853 (1996).
- 15. L. D. Marks, J. Cryst. Growth 61, 556 (1983).
- 16. L. D. Marks, Philos. Mag. A 49, 81 (1984).
- 17. S. Ino, J. Phys. Soc. Jpn. 27, 941 (1969).
- 18. J. Bühler and Y. Prior, J. Cryst. Growth 209, 779 (2000).
- 19. F. H. C. Crick and J. D. Watson, Nature 177, 473 (1956).
- A. Klug, R. E. Franklin, and S. P. F. Humphreys-Owen, *Biochim. Biophys. Acta* 32, 203 (1959).
- 21. J. T. Finch and A. Klug, Acta Crystallogr. 13, 1051 (1960).
- G. Millman, B. G. Uzman, A. Mitchell, and R. Langridge, *Science* 152, 1381 (1966).
- 23. J. L. Melnick, E. R. Rabin and A. B. Jenson, J. Virol. 2, 78 (1968).
- 24. T. L. Daulton, D. D. Eisenhour, P. R. Buseck, R. S. Lewis, and T. J. Bernatowicz, in "Abstracts of the 25th Lunar & Planetary Science Conference," p. 313. Houston, 1994.
- C. Hintze, in "Handbuch der Mineralogie. I. Elemente und Sulfide" p. 3. Verlag von Veit und Co., Leipzig, 1904.
- F. Wallerant, in "Cristallographie" (C. Beranger, Ed.), p. 117.
 Librairie Polytechnique, Paris, 1909.
- A. von Fersmann and V. Goldschmidt, in "Der Diamant" p. 204.
 Carl Winters Universitätsbuchhandlung, Heidelberg, 1911.
- V. M. Goldschmidt, in "Atlas der Kristallformen" p. Pl–48. Carl Winters Universitätsbuchhandlung, Heidelberg, 1918.
- C. Palache, H. Berman, and C. Frondel, in "The System of Mineralogy of J. D. Dana and E. S. Dana; I. Elements, Sulfides, Sulfosalts, Oxides" p. 88. John Wiley and Sons, New York, 1944.
- 30. G. Rose, Pogg. Ann. 23, 196 (1831).
- S. von Waltershausen, Nachr. Königl. Wissensch. Ges. Göttingen 135 (1863).
- 32. A. von Lasaulx, Sitzungsber. Niederrhein. Gesellsch. 39, 95 (1882).
- 33. G. von Rath, Z. Kristallogr. 1, 1 (1877).
- 34. C. Hermann, Z. Kristallogr. 79, 186 (1931).
- P. Niggli, in "Lehrbuch der Mineralogie und Kristallchemie,"
 p. 123. Verlag Gebrüder Borntraeger, Berlin, 1941.
- 36. R. L. Segall, J. Metals 9, 50 (1957).

- 37. A. J. Melmed and D. O. Hayward, J. Chem. Phys. 31, 545 (1959).
- 38. A. Mackay, Acta Crystallogr. 15, 916 (1962).
- H. Schlötterer, in "Proc. 5th Int. Congr. on Electron Microscopy"
 (S. S. Breese Jr. Ed.), p. DD6. Academic Press, New York, 1962.
- 40. H. Schlötterer, Z. Kristallogr. 119, 321 (1964).
- 41. H. Schlötterer, Metalloberfläche 18, 33 (1964).
- 42. R. H. Wentorf, in "The Art and Science of Growing Crystals" (J. Gilman, Ed.), p. 176. J. Wiley & Sons, New York, 1963.
- 43. J. W. Faust and H. F. John, J. Phys. Chem. Solids 25, 1407 (1964).
- 44. D. C. Skillman and C. R. Berry, Photogr. Sci. Eng. 1964, 65 (1964).
- F. Ogburn, B. Paretzkin, and H. S. Peiser, Acta Crystallogr. 17, 774 (1964).
- J. Smit, F. Ogburn, and C. J. Bechtold, J. Electrochem. Soc. 115, 371 (1968).
- 47. R. L. Schwoebel, Surf. Sci. 2, 356 (1964).
- 48. R. L. Schwoebel, J. Appl. Phys. 37, 2515 (1966).
- M. A. Gedwill, C. J. Altstetter and C. M. Wayman, J. Appl. Phys. 35, 2266 (1964).
- 50. R. W. DeBlois, J. Appl. Phys. 36, 1647 (1965).
- 51. R. W. DeBlois, J. Vac. Sci. Technol. 3, 146 (1966).
- 52. B. G. Bagley, Nature 208, 674 (1965).
- 53. J. A. R. Clarke and J. D. Bernal, Nature 211, 280 (1966).
- 54. B. G. Bagley, J. Cryst. Growth 6, 323 (1970).
- 55. G. L. Downs and J. D. Braun, Science 154, 1443 (1966).
- J. G. Allpress, H. Jaeger, P. D. Mercer, and J. V. Sanders, in "Proc.
 Int. Congr. on Electron Microscopy" (R. Uyeda, Ed.), p. 489.
 Maruzen Co. Ltd., Tokyo, 1966.
- 57. J. G. Allpress and J. V. Sanders, Surf. Sci. 7, 1 (1967).
- M. Gillet and E. Gillet, in "Proc. 6. Int Congr. on Electron Microscopy" (R. Uyeda, Ed.), p. 633. Maruzen Co. Ltd., 1966.
- 59. S. Ino, J. Phys. Soc. Jpn. 21, 346 (1966).
- S. Ino and S. Ogawa, in "Proc. 6. Int Congr. on Electron Microscopy" (R. Uyeda, Ed.), p. 521. Maruzen Co. Ltd., Tokyo, 1966.
- 61. S. Ino and S. Ogawa, J. Phys. Soc. Jpn. 22, 1365 (1967).
- S. Ogawa, D. Watanabe, S. Ino, T. Kato, and H. Ota, Sci. Rep. Res. Inst. Tohoku Univ. A 18 Suppl., 171 (1966).
- S. Ogawa, S. Ino, T. Kato, and H. Ota, J. Phys. Soc. Jpn. 21, 1963 (1966).
- 64. K. Kimoto and I. Nishida, Jpn. J. Appl. Phys. 6, 1047 (1967).
- G. Rupprechter, K. Hayek, and H. Hofmeister, J. Catal. 173, 409–422 (1998).
- P. Melinon, G. Fuchs and M. Treilleux, J. Phys. I (France) 2, 1263 (1992).
- L. R. Wallenberg, J. O. Bovin, and G. Schmid, Surf. Sci. 156, 256 (1985).
- 68. S. Iijima and T. Ishihashi, Phys. Rev. Lett. 56, 616 (1986).
- D. J. Smith, A. K. Petford-Long, R. Wallenberg, and J. O. Bovin, Science 233, 872 (1986).
- L. R. Wallenberg, J. O. Bovin, A. K. Petford-Long, and D. J. Smith, *Ultramicroscopy* 20, 71 (1986).
- J. O. Malm, J. O. Bovin, A. Petford-Long, D. J. Smith, G. Schmid, and N. Klein, Angew. Chem., Int. Ed. 27, 555 (1988).
- D. Shechtman, I. Blech, D. Gratias, and J. W. Cahn, *Phys. Rev. Lett.* 53, 1951 (1984).
- 73. D. Levine and P. J. Steinhardt, Phys. Rev. Lett. 53, 2477 (1984).
- K. Hiraga, M. Hirabayashi, A. Inoue, and T. Masumoto, Sci. Rep. Res. Inst. Tohoku Univ. A 32, 309 (1985).
- 75. D. R. Nelson, Sci. Am. 254, 42 (1986).
- 76. D. R. Nelson and B. I. Halperin, Science 229, 233 (1985).
- 77. K. H. Kuo, J. de Physique Colloque C3 47, 425 (1986).
- K. H. Kuo, J. Electron Microsc. Techn. 7, 277 (1987).
 K. F. Fung, X. D. Zuo, and C. Y. Yang, Phil. Mag. 55, 27 (1987).
- W. J. Jiang, Z. K. Hei, Y. X. Guo, and K. H. Kuo, *Philos. Mag.* 52, L53 (1985).
- 81. T. R. Anantharaman, Current Science 58, 1067 (1989).
- 82. A. K. Srivastava and S. Ranganathan, Acta Mater. 44, 2935 (1996).

- 83. U. Dahmen and K. H. Westmacott, Science 233, 875 (1986).
- J. Douin, U. Dahmen, and K. H. Westmacott, Coll. Phys. C1 51, 809 (1990).
- J. Douin, U. Dahmen, and K. H. Westmacott, *Philos. Mag. B* 63, 867 (1991).
- S. Q. Xiao, S. Hinderberger, K. H. Westmacott, and U. Dahmen, Philos. Mag. A 73, 1261 (1996).
- D. Mitlin, U. Dahmen, V. Radmilovic, and J. W. Morris Jr., Mater. Sci. *Eng.*, A 301, 231 (2001).
- 88. Y. T. Pei and J. T. M. de Hosson, Acta Mater. 49, 561 (2001).
- M. Fujimoto, K. Hoshi, M. Nakazawa, and S. Sekiguchi, *Jpn. J. Appl. Phys.* 32, 5532 (1993).
- 90. M. Dubiel, H. Hofmeister, and J. Hopfe, Beitr. Elektronen-mikroskop. Direktabb. Oberfl. 24, 49 (1991).
- 91. S. T. Selvan, Y. Ono, and M. Nogami, Mater. Lett. 37, 156 (1998).
- W. Vogel, J. Bradley, O. Vollmer, and I. Abraham, J. Phys. Chem. B 102, 10853 (1998).
- F. Dassenoy, M. J. Casanove, P. Lecante, M. Verelst, E. Snoeck, A. Mosset, T. O. Ely, C. Amiens, and B. Chaudret, J. Chem. Phys. 112, 8137 (2000).
- 94. G. L. Tan, H. Hofmeister, and M. Dubiel, in "Proceedings of Autumn School on Materials Sciences and Electron Microscopy 2000" (D. S. Su and S. Wrabetz, Eds.), p. 67. FHI Berlin, Berlin-Dahlem, 2000.
- W. K. Choi, Y. W. Ho, S. P. Ng, and V. Ng, J. Appl. Phys. 89, 2168 (2001).
- M. Klimenkov, W. Matz, S. A. Nepijko, and M. Lehmann, Nucl. Instr. Methods Phys. Res., Sect. B 179, 209 (2001).
- 97. H. Hofmeister, Mater. Sci. Forum 312-314, 325 (1999).
- 98. A. Nohara, S. Ino and S. Ogawa, Jpn. J. Appl. Phys. 7, 1144 (1968).
- 99. S. Ino, J. Electron Microsc. 18, 237 (1969).
- 100. K. Reichelt and S. Schreiber, Surf. Sci. 43, 644 (1974).
- 101. Y. Fukano, Jpn. J. Appl. Phys. 13, 1001 (1974).
- 102. M. Takahashi, T. Suzuki, H. Kushima, and S. Ogasawara, Jpn. J. Appl. Phys. 17, 1499 (1978).
- 103. A. Renou, PhD Thesis, University Aix-Marseille III (1979).
- 104. M. Gillet, A. Renou, and J. M. Miquel, in "Growth and Properties of Metal Clusters" (J. Bourdon, Ed.), p. 185. Elsevier, New York, 1980.
- 105. L. D. Marks and D. J. Smith, J. Microsc. 130, 249 (1983).
- 106. Y. Ohtsuka, Acta Crystallogr. Sect. A 40, C (1984).
- 107. H. Hofmeister, Z. Phys. D 19, 307 (1991).
- 108. G. Rupprechter, K. Hayek, and H. Hofmeister, Vacuum 46, 1035 (1995).
- 109. M. Tanaka, M. Takeguchi, and K. Furuya, Surf. Sci. 433–435, 491 (1999).
- Y. Wu, Q. Chen, Ma. Takeguchi, and K. Furuya, Surf. Sci. 462, 203 (2000).
- 111. Y. Oshima, T. Nannguo, H. Hirayama, and K. Takayanagi, Surf. Sci. 476, 107 (2001).
- 112. S. Mader, J. Vac. Sci. Technol. 8, 247 (1971).
- 113. N. G. Nakhodkin, Y. A. Barabanenkov, A. F. Bardamid, A. I. Novoselskaya, and K. I. Yakimov, *Ukrainian Fiz. Zh.* 34, 1355 (1989).
- 114. V. Bykov, H. Hofmeister, T. Junghanns, and S. Nepijko, in "Proc 7. Oxford Conf. on Microscopy of Semiconducting Materials" (A. G. Cullis and N. J. Long, Eds.), p. 51. IOP Publishing Ltd., Bristol, 1991
- 115. H. Hofmeister, A. F. Bardamid, T. Junghanns, and S. A. Nepijko, Thin Solid Films 205, 20 (1991).
- 116. T. Okabe, Y. Kagawa, and S. Takai, Philos. Mag. Lett. 63, 233 (1991).
- H. Hofmeister and T. Junghanns, *Mater. Sci. Forum* 113–115, 631 (1993).
- 118. H. Hofmeister and T. Junghanns, Nanostruct. Mater. 3, 137 (1993).
- 119. H. Hofmeister and T. Junghanns, Trans. Mater. Res. Soc. Japan 16B, 1581 (1994).

- 120. H. Hofmeister and T. Junghanns, J. Non-Crystalline Solids 192 & 193, 550 (1995).
- 121. W. Neumann, H. Hofmeister, D. Conrad, K. Scheerschmidt, and S. Ruvimov, Z. Kristallogr. 211, 147 (1996).
- 122. J. G. Zheng, X. Q. Pan, M. Schweizer, F. Zhou, U. Weimar, W. Göpel, and M. Rühle, J. Appl. Phys. 79, 7688 (1996).
- 123. C. Leclercq, H. Batis, and M. Boudeulle, J. Microsc. Spectrosc. Electron. 8, 243 (1983).
- 124. Y. Saito, Y. Ishikawa, A. Oshita, H. Shinohara, and H. Nagashima, Phys. Rev. B 46, 1846 (1992).
- 125. M. Haluska, H. Kuzmany, M. Vybornov, P. Rogl, and P. Fejdi, Appl. Phys. A 56, 161 (1993).
- 126. W. L. Zhou, W. Zhao, K. K. Fung, L. Q. Chen, and Z. B. Zhang, Physica C 214, 19 (1993).
- 127. H. Kawada, Y. Fujii, H. Nakao, Y. Murakami, T. Watanuki, H. Suematsu, K. Kikuchi, Y. Achiba, and I. Ikemoto, *Phys. Rev. B* 51, 8723 (1995).
- 128. Y. Kim, L. Jiang, T. Iyoda, K. Hashimoto, and A. Fujishima, Appl. Surf. Sci. 130–132, 602 (1998).
- 129. S. Matsumoto and Y. Matsui, J. Mater. Sci. 18, 1785 (1983).
- Y. H. Lee, P. D. Richards, K. J. Bachmann, and J. T. Glass, *Appl. Phys. Lett.* 56, 620 (1990).
- D. Dorignac, S. Delclos, and F. Phillipp, *Philos. Mag. B* 81, 1879 (2001).
- 132. T. Oku and K. Hiraga, Diamond Relat. Mater. 10, 1398 (2001).
- 133. J. Narayan, A. R. Srivatsa, M. Peters, S. Yokota. and K. V. Ravi, Appl. Phys. Lett. 53, 1823 (1988).
- 134. J. Narayan, J. Mater. Res. 5, 2414 (1990).
- 135. C. Wild, N. Herres, and P. Koidl, J. Appl. Phys. 68, 973 (1990).
- 136. B. E. Williams, J. T. Glass, R. F. Davis, and K. J. Kobashi, J. Cryst. Growth 99, 1168 (1990).
- J. F. DeNatale, A. B. Harker, and J. F. Flintoff, J. Appl. Phys. 69, 6456 (1991).
- 138. J. L. Hutchison and D. Shechtman, in "Proc. EUREM92" (A. Lopéz-Galindo and M. Rodríguez-Garcia, Eds.), p. 713. Secretariado de Publicaciones de la Universidad de Granada, Granada, 1992.
- 139. D. Shechtman, J. L. Hutchison, L. H. Robins, E. N. Farabaugh, and A. Feldman, J. Mater. Res. 8, 473 (1993).
- 140. P. Wurzinger, M. Joksch, and P. Pongratz, in "Proc. Microsc. Semicond. Mater. Conf." (A. G. Cullis, A. E. Staton-Bevan, and J. L. Hutchison, Eds.), p. 157. IOP Publ., Bristol, 1993.
- 141. C. H. Chu and M. H. Hon, Mater. Chem. Phys. 38, 131 (1994).
- 142. S. Barrat and E. Bauer-Grosse, Diamond Relat. Mater. 4, 419 (1995).
- 143. J.-H. Choi, S.-H. Lee, and J.-W. Park, Mater. Chem. Phys. 45, 176 (1996).
- 144. W. N. Wang, N. A. Fox, T. J. Davis, D. Richardson, G. M. Lynch, J. W. Steeds, and J. S. Lee, *Appl. Phys. Lett.* 69, 2825 (1996).
- 145. C.-S. Yan and Y. K. Vohra, Diamond Relat. Mater. 8, 2022 (1999).
- 146. S. Delclos, D. Dorignac, F. Phillipp, F. Silva, and A. Gicquel, Diamond Relat. Mater. 9, 346 (2000).
- 147. H. Hofmeister, J. Dutta, and H. Hofmann, Phys. Rev. B 54, 2856 (1996).
- 148. J. Dutta, R. Houriet, H. Hofmann, and H. Hofmeister, Nanostruct. Mater. 9, 359 (1997).
- 149. W. Qin, D. G. Ast, and T. I. Kamins, Jpn. J. Appl. Phys. 40, 4806 (2001).
- 150. T. N. Millers and A. A. Kuzjukévics, Prog. Cryst. Growth & Charact. Mat. 16, 367 (1988).
- 151. H. E. Cheng and H. M. Hon, J. Cryst. Growth 142, 117 (1994).
- 152. H. E. Cheng, T. T. Lin, and M. H. Hon, Scripta Mater. 36, 113 (1996).
- 153. W. P. Sun, D. J. Cheng, and M. H. Hon, J. Cryst. Growth 71, 787 (1985).
- 154. D. J. Cheng, W. P. Sun, and M. H. Hon, *Thin Solid Films* 146, 45
- 155. F. Ernst and P. Pirouz, J. Appl. Phys. 64, 4526 (1988).

- 156. G. Turner and E. Bauer, in "Proc. 5. Int. Cong. Electron Microsc." (S. S. Breese Jr., Ed.), p. DD3. Academic Press, New York, 1962.
- 157. N. Wada, Jpn. J. Appl. Phys. 7, 1287 (1968).
- 158. R. Uyeda, J. Cryst. Growth 24/25, 69 (1974).
- 159. T. Hayashi, T. Ohno, S. Yatsuya, and R. Uyeda, Jpn. J. Appl. Phys. 16, 705 (1977).
- 160. T. Ohno and K. Yamauchi, Jpn. J. Appl. Phys. 20, 1385 (1981).
- 161. A. Renou and M. Gillet, Surf. Sci. 106, 27 (1981).
- 162. M. Arita, N. Suzuki, and I. Nishida, Nagoya University Research Bulletin B 37, 39 (1993).
- 163. J. Urban, H. Sack-Kongehl, and K. Weiss, Catal. Lett. 49, 101 (1997).
- 164. M. Hyslop, A. Wurl, S. A. Brown, B. D. Hall, and R. Monot, Eur. Phys. J. D 16, 233 (2001).
- 165. B. Rellinghaus, S. Stappert, E. F. Wassermann, H. Sauer, and B. Spliethoff, Eur. Phys. J. D 16, 249 (2001).
- 166. H. Hofmeister, S. A. Nepijko, D. N. Ievlev, W. Schulze, and G. Ertl, J. Cryst. Growth 234, 773 (2002).
- 167. B. Q. Wei, R. Vajtai, Y. J. Jung, F. Banhart, G. Ramanath, and P. M. Ajayan, J. Phys. Chem. B 106, 5807 (2002).
- 168. Y. Saito, J. Cryst. Growth 47, 61 (1979).
- 169. S. Iijima, Jpn. J. Appl. Phys. 26, 365 (1987).
- D. K. Saha, K. Koga, and H. Takeo, *Nanostruct. Mater.* 8, 1139 (1997).
- 171. S. Stappert, B. Rellinghaus, M. Acet, and E. Wassermann, in "Nanoparticulate Materials" (R. K. Singh, R. Partch, M. Muhammed, M. Senna, and H. Hofmann, Eds.), p. 73. MRS, Warrendale, PA, 2002.
- 172. Y. Saito, S. Yatsuya, K. Mihama, and R. Uyeda, Jpn. J. Appl. Phys. 17, 1149 (1978).
- 173. P. Gao, Z. Phys. D 15, 175 (1990).
- 174. C. Altenhein, S. Giorgio, J. Urban, and K. Weiss, J. Phys. D 19, 303 (1991).
- 175. M. Flüeli, R. Spycher, P. Stadelmann, Ph. Buffat, and J. P. Borel, J. Microsc. Spectrosc. Electron. 14, 351 (1989).
- 176. B. Hall, PhD Thesis, EPFL Lausanne, (1991).
- 177. D. Reinhard, B. D. Hall, D. Ugarte, and R. Monod, Z. Phys. D 26 Suppl., 76 (1993).
- 178. D. Reinhard, B. D. Hall, P. Berthoud, S. Valkealathi, and R. Mono, Phys. Rev. B 58, 4917 (1998).
- 179. S. W. Yu, G. H. Wang, S. Y. Yin, Y. X. Zhang, and Z. G. Liu, Phys. Lett. A 268, 442 (2000).
- 180. F. Ding, G. Wang, S. Yu, J. Wang, W. Shen, and H. Li, Eur. Phys. J. D 16, 245 (2001).
- 181. J.-P. Barnes, A. K. Petford-Long, R. C. Doole, R. Serna, J. Gonzalo, A. Suárez-García, C. N. Afonso, and D. Hole, Nanotechnology 13, 465 (2002).
- 182. R. A. Roy, R. Messier, and J. M. Cowley, Thin Solid Films 79, 207 (1981).
- 183. E. Bouzy, G. Le Caer, and E. Bauer-Grosse, *Philos. Mag. Lett.* 64, 1 (1991).
- 184. H. Hubert, B. Devouard, L. A. J. Garvie, M. O'Keefe, P. R. Buseck, W. T. Petuskey, and P. F. McMillan, Nature 391, 376 (1998).
- 185. H. Fredriksson, M. Hillert, and N. Lange, J. Inst. Metals 101, 285 (1973).
- 186. K. Kobayashi and L. M. Hogan, Philos. Mag. A 40, 399 (1979).
- 187. J. J. Hu and P. L. Ryder, Philos Mag. 68, 389 (1993).
- 188. M. Ellner and U. Burkhardt, J. Alloys Compd. 198, 91 (1993).
- 189. N. Uyeda, M. Nishino, and E. Suito, J. Colloid Interface Sci. 43, 264 (1973).
- 190. M. Brieu and M. Gillet, Thin Solid Films 100, 53 (1983).
- 191. N. J. Long, R. F. Marzke, M. McKelvy, and W. S. Glausinger, Ultramicroscopy 20, 15 (1986).
- 192. M. Brieu and M. Gillet, Thin Solid Films 167, 149 (1988).
- 193. A. C. Curtis, D. G. Duff, P. P. Edwards, D. A. Jefferson, B. F. G. Johnson, A. I. Kirkland, and A. S. Wallace, J. Phys. Chem. B 92, 2270 (1988).

- 194. D. G. Duff, P. P. Edwards, J. Evans, J. T. Gauntlett, D. A. Jefferson, B. F. G. Johnson, A. I. Kirkland, and D. J. Smith, Ang. Chem., Int. Ed. 28, 590 (1989).
- 195. W. Vogel, D. G. Duff, and A. Baiker, Langmuir 11, 401 (1995).
- 196. G. M. Chow, M. A. Markowitz, R. Rayne, D. N. Dunn, and A. Singh, J. Colloid Interface Sci. 183, 135 (1996).
- 197. C. Greffié, M. F. Benedetti, C. Parron, and M. Amouric, *Geochim. Cosmochim. Acta* 60, 1531 (1996).
- 198. Q. Li, M. Shao, S. Zhang, X. Liu, G. Li, K. Jiang, and Y. Qian, J. Cryst. Growth 243, 327–330 (2002).
- 199. R. Breckpot, Anales Real Soc. Esp. Fisica y Quimica B 51, 31 (1965).
- 200. I. Epelboin, M. Froment, and G. Maurin, Plating 56, 1356 (1969).
- I. Epelboin, M. Froment, and G. Maurin, in "Electrocystallization; Proc. 28. Meeting Int. Soc. Electrochem" p. 371. Varna, 1977.
- 202. C. R. Hall and S. A. H. Fawzi, Philos. Mag. A 54, 805 (1986).
- M. Froment and G. Maurin, J. Microsc. Spectrosc. Electron. 12, 379 (1987).
- 204. H. Hofmeister and N. Atanassov, in "Proceedings of the 11th European Conference on Electron Microscopy, Dublin 1996" (Committee of Europ. Soc. of Microsc., Ed.), p. 333. Brussels, 1998.
- 205. N. Pangarov and V. Velinov, Electrochim. Acta 13, 1641 (1968).
- 206. M. Froment and J. Thevenin, Metaux Corros. Ind. 54, 43 (1975).
- C. Digard, M. Maurin, and J. Robert, *Metaux Corros. Ind.* 51, 255 (1976).
- 208. J. Thevenin and M. Froment, *J. Microsc. Spectrosc. Electron.* 1, 7 (1976).
- D.-L. Lu, Y. Okawa, K. Suzuki, and K.-I. Tanaka, Surf. Sci. 325, L397 (1995).
- 210. D.-L. Lu and K.-I. Tanaka, J. Solid State Electrochem 1, 187 (1997).
- V. Radmilovic, K. I. Popov, M. G. Pavlovic, A. Dimitrov, and S. H. Jordanov, J. Sol. State Electrochem. 2, 162 (1998).
- B. Bozzine, A. Fanigliulo, and M. Serra, J. Cryst. Growth 231, 589 (2001).
- 213. D.-L. Lu, K. Domen, and K.-I. Tanaka, Langmuir 18, 3226 (2002).
- 214. D.-L. Lu, Y. Okawa, M. Ichihara, A. Aramata, and K. Tanaka, J. Electroanal. Chem. 406, 101 (1996).
- 215. D.-L. Lu and K. Tanaka, Phys. Rev. B 55, 13865 (1997).
- 216. D.-L. Lu and K.-I. Tanaka, J. Cryst. Growth 181, 395 (1997).
- 217. P. Claus and H. Hofmeister, J. Phys. Chem. B 103, 2766 (1999).
- K. Chattopadhay and P. Ramachandrarao, J. Cryst. Growth 36, 355 (1976).
- 219. M. D. Ball and D. J. Lloyd, Scr. Met. 19, 1065 (1985).
- 220. H. Hofmeister, Cryst. Res. Technol. 33, 3 (1998).
- 221. H. Hofmeister, W. G. Drost, and A. Berger, *Nanostruct. Mater.* 12, 207 (1999).
- C. Mohr, M. Dubiel and H. Hofmeister, J. Phys.: Condens. Matter 13, 525 (2001).
- 223. H. Hofmeister and U. Kahler, in "Silicon Chemistry: From Molecules to Extended Systems" (P. Jutzi and U. Schubert, Eds.), Wiley-VCH, Weinheim (2003), in print.
- 224. H. Hofmeister, P. Werner, and T. Junghanns, in "Physics and Chemistry of Finite Systems: From Clusters to Crystals" (P. Jena, S. N. Khanna, and B. K. Rao, Eds.), p. 1251. Kluwer Academic Publ., Dordrecht, 1992.
- 225. A. Nohara and T. Imura, J. Phys. Soc. Jpn. 27, 793 (1969).
- 226. G. Rupprechter, G. Seeber, K. Hayek, and H. Hofmeister, *Phys. Status Solidi A* 146, 449 (1994). 213, 86 (2003)
- 227. C. Mohr, H. Hofmeister, and P. Claus, J. Catal. XXX, yyy (2002).
- 228. Y. Matsui, J. Cryst. Growth 66, 243 (1984).
- 229. J. O. Malm, G. Schmid, and B. Morun, Philos. Mag. 63, 487 (1991).
- P. J. Herley and W. Jones, J. Chem. Soc. Faraday Trans. 88, 3213 (1992).
- P. J. Herley, N. P. Fitzsimons, and W. Jones, J. Chem. Soc. Faraday Trans. 91, 719 (1995).
- 232. B. S. Xu and S.-I. Tanaka, Nanostruct. Mater. 8, 1131 (1997).

- 233. S. Thiel, M. Dubiel, S. Schurig, and H. Hofmeister, in "Proceedings of the 11th European Conference on Electron Microscopy, Dublin 1996" Committee of Europ. Soc. of Microsc., Brussels, 1998, p. 445.
- 234. M. Takeguchi, M. Tanaka, H. Yasuda, and K. Furuya, Surf. Sci. 493, 414 (2001).
- T. Takami, K.-I. Sugiura, Y. Sakata, T. Takeuchi, and S. Ino, *Appl. Surf. Sci.* 130–132, 834 (1998).
- 236. T. Takami, M. Brause, D. Ochs, W. Maus-Friedrichs, V. Kempter, and S. Ino, Surf. Sci. 407, 140 (1998).
- 237. S. Ogawa and S. Ino, J. Vac. Sci. Technol. 6, 527 (1969).
- 238. H. Sato and S. S. Shinozaki, J. Appl. Phys. 41, 3165 (1970).
- 239. S. Ogawa and S. Ino, J. Cryst. Growth 13/14, 48 (1972).
- 240. E. Gillet and M. Gillet, J. Cryst. Growth 13/14, 212 (1972).
- 241. P. F. McMillan, H. Hubert, A. Chizmeshya, W. T. Petuskey, L. A. J. Garvie, and B. Devouard, J. Solid State Chem. 147, 281 (1999).
- 242. T. P. Martin, T. Bergmann, H. Göhlich, and T. Lange, *Chem. Phys. Lett.* 176, 343 (1991).
- 243. T. P. Martin, T. Bergmann, H. Göhlich, and T. Lange, Z. Phys. D 19, 25 (1991).
- 244. T. P. Martin, T. Bergmann, H. Göhlich, and T. Lange, J. Phys. Chem. B 95, 6421 (1991).
- 245. J. Uppenbrink and D. J. Wales, J. Chem. Soc. Faraday Trans. 87, 215 (1991).
- 246. J. Uppenbrink and D. J. Wales, J. Chem. Phys. 96, 8520 (1992).
- 247. J. P. K. Doye and D. J. Wales, Chem. Phys. Lett. 247, 339 (1995).
- 248. J. P. K. Doye, D. J. Wales, and R. S. Berry, J. Chem. Phys. 103, 4234 (1995).
- 249. V. V. Volkov, G. van Tendeloo, G. A. Tsirkov, N. V. Cherkashina, M. N. Vargaftik, I. I. Moiseev, V. M. Novotortsev, A. V. Kvit, and A. L. Chuvilin, J. Cryst. Growth 163, 377 (1996).
- 250. C. Gerstengarbe and W. Neumann, in "Publications of the 12th Electron Microscopy Conference" (J. Heydenreich and H. Luppa, Eds.), p. 481. Dresden, 1988.
- 251. H. Hofmeister, Phys. Bl. 53, 37 (1997).
- 252. L. A. Paquette, D. W. Balogh, R. Usha, D. Kountz, and G. G. Christoph, *Science* 211, 575 (1981).
- 253. H. Hofmeister, in "Nanophase Materials, NATO ASI Series E" (G. C. Hadjipanayis and R. W. Siegel, Eds.), p. 209. Kluwer Academic Publ., Dordrecht, 1994.
- 254. E. Gillet and M. Gillet, Thin Solid Films 4, 171 (1969).
- 255. G. Honjo and Yagi K, J. Vac. Sci. Technol. 6, 576 (1969).
- 256. J. G. Allpress and J. V. Sanders, Austral. J. Physics 23, 23 (1970).
- S. A. Nepijko, V. I. Styopkin, and R. Scholz, *Poverchnostj* 4, 116 (1984).
- 258. K. Yagi, K. Takayanagi, K. Kobayashi, and G. Honjo, J. Cryst. Growth 28, 117 (1975).
- 259. H. Hofmeister, Thin Solid Films 116, 151 (1984).
- 260. S. A. H. Fawzi. PhD Thesis, University of Warwick (1984).
- 261. B. W. van de Waal, J. Cryst. Growth 158, 153 (1996).
- 262. B. W. van de Waal, Phys. Rev. Lett. 76, 1083 (1996).
- 263. B. W. van de Waal, PhD Thesis, University of Twente (1997).
- 264. M. S. Abrahams, J. L. Hutchison, and G. K. Booker, *Phys. Status Solidi A* 63, K3 (1981).
- 265. C. Gerstengarbe and W. Neumann, in "Publications of the 11th Electron Microscopy Conference" (J. Heydenreich and H. Luppa, Eds.), p. 253. Dresden, 1984.
- 266. K. C. Paus, J. C. Barry, G. R. Brooker, T. B. Peters, and M. G. Pitt, in "Proc. Micros. Semicond. Mater. Conf." (A. G. Cullis and D. B. Holt, Eds.), p. 35. Adam Hilger, Bristol, 1985.
- 267. W. Wegscheider, K. Eberl, G. Abstreiter, H. Cerva, and H. Oppolzer, *Appl. Phys. Lett.* 57, 1496 (1990).
- 268. G. Wagner and P. Paufler, Z. Kristallogr. 195, 17 (1991).
- D. M. Hwang, S. A. Schwarz, T. S. Ravi, R. Bhat, and C. Y. Chen, *Phys. Rev. Lett.* 66, 739 (1991).
- 270. W. Wegscheider, K. Eberl, G. Abstreiter, H. Cerva and H. Oppolzer, in "Proc. 7th Oxford Conf. Microsc. Semicond.

- Mater." (N. J. Long and A. G. Cullis, Eds.), p. 21. IOP Publishing Ltd., Bristol, 1991.
- 271. D. J. Smith and L. D. Marks, J. Cryst. Growth 54, 433 (1981).
- 272. L. D. Marks, Thin Solid Films 136, 309 (1986).
- 273. H. Hofmeister and T. Junghanns, in "Proc. Autumn School1991 of the Int. Centre of Electron Microsc." (J. Heydenreich and W. Neumann, Eds.), p. 245. MPI Halle, Halle, 1992.
- S. Krafczyk, H. Jacobi, and H. Follner, *Cryst. Res. Technol.* 32, 163 (1997).
- 275. J. Farges, M. F. de Feraudey, B. Raoult, and G. Torchet, *Acta Crystallogr. A* 38, 656 (1982).
- J. Farges, M. F. de Feraudy, B. Raoult, and G. Torchet, *J. Chem. Phys.* 78, 5067 (1983).
- J. Farges, M. F. de Feraudy, B. Raoult, and G. Torchet, *J. Chem. Phys.* 84, 3491 (1986).
- J. Farges, M. F. de Feraudy, B. Raoult, and G. Torchet, *Adv. Chem. Phys.* 70, 45 (1988).
- 279. B. Raoult, J. Farges, M. F. de Feraudy, and G. Torchet, *Philos. Mag. B* 60, 881 (1989).
- 280. B. W. van de Waal, J. Chem. Phys. 90, 3407 (1989).
- 281. B. W. van de Waal, J. Chem. Phys. 98, 4909 (1993).
- M. B. Gordon, F. Cyrot-Lackmann, and M. C. Desjonqueres, Surf. Sci. 80, 159 (1979).
- 283. R. Mosserri and J. F. Sadoc, Z. Phys. D 12, 89 (1989).
- 284. C. L. Cleveland and U. Landman, J. Chem. Phys. 94, 7376 (1991).
- 285. J.-Y. Yi, D. J. Oh and J. Bernholc, Phys. Rev. Lett. 67, 1594 (1991).
- Q. Wang, M. D. Glossmann, M. P. Iniguez, and J. A. Alonso, *Philos. Mag. B* 69, 1045 (1994).
- D. J. Wales, L. J. Munro, and J. P. K. Doye, *J. Chem. Soc., Dalton Trans.* 5, 611 (1996).
- 288. Y. J. Lee, J. Y. Maeng, E. K. Lee, B. Kim, S. Kim, and K. K. Han, J. Comput. Chem. 21, 380 (2000).
- F. Baletto, R. Ferrando, A. Fortunelli, F. Montaleni, and C. Mottet, J. Chem. Phys. 116, 3856 (2002).
- B. D. Hall, M. Flueli, R. Monot, and J.-P. Borel, Z. Phys. D 12, 97 (1989).
- 291. B. D. Hall, M. Flueli, R. Monot, and J. P. Borel, *Phys. Rev. B* 43, 3906 (1991).
- 292. D. Reinhard, R. D. Hall, D. Ugarte, and R. Monod, *Phys. Rev. B* 55, 7868 (1997).
- 293. M. Pellarin, B. Baguenard, J. L. Valle, J. Lerme, M. Broyer, J. Miller, and A. Perez, Chem. Phys. Lett. 217, 349 (1994).
- 294. T. P. Martin, Phys. Rep. 273, 199 (1996).
- 295. B. M. Smirnov, Chem. Phys. Lett. 232, 395 (1995).
- J. P. K. Doye and D. J. Wales, J. Chem. Soc. Faraday Trans. 93, 4233 (1997).
- T. Ikeshoji, G. Torchet, M.-F. de Feraudy, and K. Koga, *Phys. Rev.* B 63, 031101 (2001).
- 298. M. R. Hoare and P. Pal, Adv. Phys. 20, 161 (1971).
- 299. J. J. Burton, in "Materials Science Research" (G. C. Kuczynski, Ed.), p. 17. Plenum Press, New York, 1975.
- J. Xie, J. A. Northby, D. L. Freeman, and J. D. Doll, *J. Chem. Phys.* 91, 612 (1989).
- 301. A. Sachdev and R. I. Masel, J. Mater. Res. 8, 455 (1993).
- 302. A. Sachdev, R. I. Masel, and J. B. Adams, Z. Phys. D 26, 310 (1993).
- I. G. Garzón and A. Posada-Amarillas, *Phys. Rev. B* 54, 11796 (1996).
- 304. C. L. Cleveland, U. Landman, M. N. Shafigullin, P. W. Stephens, and R. L. Whetten, Z. Phys. D 40, 503 (1997).
- C. L. Cleveland, U. Landman, T. G. Schaaff, M. N. Shafigullin,
 P. W. Stephens, and R. L. Whetten, *Phys. Rev. Lett.* 79, 1873 (1997).
- I. L. Garzón, K. Michaelian, M. R. Beltrán, A. Posada-Amarillas,
 P. Ordejón, E. Artacho, D. Sánchez-Portal, and J. M. Soler, *Eur. Phys. J. D* 9, 211 (1999).
- L. G. Gonzalez and J. M. Montejano-Carrizales, *Phys. Status Solidi B* 220, 357 (2000).

- 308. J. L. Aragón, Chem. Phys. Lett. 226, 263 (1994).
- R. S. Berry, B. M. Smyrnov, and A. Y. Strizhev, *J. Exp. Theor. Phys.* 85, 588 (1997).
- C. L. Cleveland, W. D. Luedtke, and U. Landman, *Phys. Rev. Lett.* 81, 2036 (1998).
- F. Baletto, C. Mottet, and R. Ferrando, *Phys. Rev. Lett.* 84, 5544 (2000).
- 312. C. Barreteau, M. C. Desjonquères, and D. Spanjaard, Eur. Phys. J. D 11, 395 (2000).
- L. Vitos, B. Johansson, and J. Kollar, *Phys. Rev. B* 62, R11957 (2000).
- 314. W. H. Zhang, L. Liu, J. Zhuang, and Y. F. Li, Phys. Rev. B 62, 8276 (2000).
- 315. F. Baletto and R. Ferrando, Surf. Sci. 490, 361 (2001).
- 316. F. Baletto, C. Mottet, and R. Ferrando, *Eur. Phys. J. D* 16, 25 (2001).
- C. L. Cleveland, W. D. Luedtke, and U. Landman, *Phys. Rev. B* 60, 5065 (1999).
- 318. I. G. Garzón, K. Michaelian, M. R. Beltrán, A. Posada-Amarillas, P. Ordejón, E. Artacho, D. Sánchez-Portal, and J. M. Soler, *Phys. Rev. Lett.* 81, 1600 (1998).
- 319. F. Baletto, J. P. K. Doye, and R. Ferrando, Phys. Rev. Lett. 88, 075503 (2002).
- 320. P. M. Ajayan and L. D. Marks, Phase Transitions 24-26, 229 (1990).
- 321. N. Doraiswamy and L. D. Marks, Philos. Mag. B 71, 291 (1995).
- S. Iijima, in "Proc. XI. Int. Cong. on Electron Microsc." (T. Imura, S. Maruse, and T. Suzuki, Eds.), p. 87. The Japanese Society of Electron Microscopy, Tokyo, 1986.
- 323. K. Harada, H. Endoh, and R. Shimizu, Technol. Reports Osaka Univ. 37, 221 (1987).
- 324. S. Iijima, in "Microclusters" (Y. Nishina, S. Ohnishi, and S. Sugano, Eds.), p. 186. Springer-Verlag, Berlin, 1987.
- 325. L. R. Wallenberg, PhD Thesis, University of Lund (1987).
- 326. M. Mitome, Y. Tanishiro, and K. Takayanagi, Z. Phys. D 12, 45 (1989).
- 327. T. Kizuka, T. Kachi, and N. Tanaka, Z. Phys. D 26 Suppl., 58 (1993).
- 328. V. G. Gryaznov, J. Heydenreich, A. M. Kaprelov, S. A. Nepijko, A. E. Romanov, and J. Urban, *Cryst. Res. Technol.* 34, 1091 (1999).
- 329. G. P. Dimitrakopulos, P. Komninou, T. Karakostas, and R. C. Pond, *Interface Science* 7, 217 (1999).
- 330. P. M. Ajayan and L. D. Marks, Phys. Rev. Lett. 60, 585 (1988).
- J. Dundurs, L. D. Marks, and P. M. Ajayan, *Philos. Mag. A* 57, 605 (1988).
- 332. A. Howie and L. D. Marks, Philos. Mag. A 49, 95 (1984).
- 333. D. Reinhard, B. D. Hall, P. Berthoud, S. Valkealathi, and R. Monod, *Phys. Rev. Lett.* 79, 1459 (1997).
- 334. C. Y. Yang, J. Cryst. Growth 47, 274 (1979).
- K. Heinemann, M. J. Yacaman, C. Y. Yang, and H. Poppa, J. Cryst. Growth 47, 177 (1979).
- 336. M. J. Yacaman, K. Heinemann, C. Y. Yang, and H. Poppa, J. Cryst. Growth 187 (1979).
- C. Y. Yang, M. J. Yacáman, and K. Heinemann, J. Cryst. Growth 47, 283 (1979).
- 338. C. Y. Yang, K. Heinemann, M. J. Yacáman, and H. Poppa, Thin Solid Films 58, 163 (1979).
- 339. M. J. Carr, J. Appl. Phys. 59, 1063 (1986).
- 340. Q. Chen, M. Tanaka, and K. Furuya, Surf. Sci. 440, 398 (1999).
- 341. H. Hubert, L. A. J. Garvie, B. Devouard, P. R. Buseck, W. T. Petuskey, and P. F. McMillan, Chem. Mater. 10, 1530 (1998).
- 342. R. I. Kostov and I. Kostov, Cryst. Res. Technol. 23, 973 (1988).
- 343. A. Mackay, Naturwissenschaften 391, 334 (1998).
- 344. I. Kostov and R. I. Kostov, in "Crystal Habits of Minerals" (M. Drinov, Ed.), p. 45. Academic Publishing House, Sofia, 1999.
- 345. P. M. Ayajan, L. D. Marks, and J. Dundurs, in "Mater. Res. Soc. Symp. Proc.," p. 469. Materials Research Society, 1987.
- 346. V. G. Gryaznov, A. M. Kaprelov, A. E. Romanov, and I. A. Polonski, *Phys. Status Solidi B* 167, 441 (1991).

- 347. O. A. Shenderova and D. W. Brenner, Phys. Rev. B 60, 7053 (1999).
- 348. L. D. Marks, Surf. Sci. 150, 302 (1985).
- 349. L. D. Marks and D. J. Smith, J. Cryst. Growth 54, 425 (1981).
- 350. N. J. Pipkin and D. J. Davies, Philos. Mag. A 40, 435 (1979).
- J. Narayan, A. R. Srivatsa, and K. V. Ravi, Appl. Phys. Lett. 54, 1659 (1989).
- 352. B. E. Williams, H. S. Kong, and J. T. Glass, *J. Mater. Res.* 5, 801 (1990).
- 353. T. Wada, T. Negami, and M. Nishitani, *Appl. Phys. Lett.* 64, 333 (1994).
- 354. D. J. Smith and L. D. Marks, Philos. Mag. A 44, 735 (1981).
- 355. K. Koga, H. Takeo, T. Ikeda, and K. Oshima, *Phys. Rev. B* 57, 4053 (1998).
- 356. K. Kimoto and I. Nishida, J. Phys. Soc. Jpn. 22, 940 (1967).
- 357. A. Renou and M. Gillet, Thin Solid Films 44, 75 (1977).
- 358. A. Gomez, P. Schabes-Retchkiman, and M. J. Yacaman, *Thin Solid Films* 98, L95 (1982).
- 359. W. Neumann and C. Gerstengarbe, in "Publications of the 11th Electron Microscopy Conference" (J. Heydenreich and H. Luppa, Eds.), p. 148. Dresden, 1984.
- 360. P. Schabes-Retchkiman, A. Gomez, G. Vazquez-Polo, and M. J. Yacaman, J. Vac. Sci. Technol. A 2, 22 (1984).
- 361. A. Renou and A. Rudra, Surf. Sci. 156, 69 (1985).
- 362. A. I. Kirkland, D. A. Jefferson, D. Tang, and P. P. Edwards, *Proc. R. Soc. London. Ser. A* 434, 279 (1991).
- 363. B. C. Smith and P. L. Gai, in "Proc. 8th Europ. Cong. Electron Microscopy" (À. Csanády, P. Röhlich, and P. Szabo, Eds.), p. 1151. Progr. Committee 8. Europ. Cong. Electron Microscopy, Budapest, 1984.
- 364. M. J. Yacamán and T. Z. Ocana, Phys. Status Solidi A 42, 571 (1977).
- H. Hofmeister, H. Haefke, and M. Krohn, J. Cryst. Growth 58, 507 (1982).
- 366. T. Komoda, Jpn. J. Appl. Phys. 7, 27 (1968).
- 367. T. Komoda, Bull. Jap. Inst. Metals 7, 661 (1968).
- 368. L. D. Marks, Ultramicroscopy 18, 445 (1985).
- 369. J. M. Penisson and A. Renou, in "Proc. Europ. Electron Microscopy Meeting," IOP Publ., Bristol, 1988.
- 370. S. Giorgio, J. Urban, and W. Kunath, *Philos. Mag. A* 60, 553 (1989).
- 371. J.-O. Bovin and J.-O. Malm, Z. Phys. D 19, 293 (1991).
- 372. D. J. Wales, A. I. Kirkland, and D. A. Jefferson, J. Chem. Phys. 91, 603 (1989).
- 373. M. J. Yacaman, R. Herrera, A. Gomez, S. Tehuacanero, and P. Schabes-Retchkiman, *Surf. Sci.* 237, 248 (1990).
- 374. M. J. Yacaman, D. Romeu, S. Fuentes, and J. M. Domingues, J. Chim. Phys. 78, 861 (1981).
- J. C. Barry, L. A. Bursill, and J. V. Sanders, *Australian J. Phys.* 38, 437 (1985).
- 376. P. L. Gai, M. J. Goringe, and J. C. Barry, J. Microsc. 142, 9 (1986).
- 377. D. G. Duff, A. C. Curtis, P. P. Edwards, D. A. Jefferson, B. F. G. Johnson, A. I. Kirkland, and D. E. Logan, *Angew. Chem.*, *Int. Ed.* 26, 676 (1987).
- 378. M. Flüeli, R. Spycher, P. A. Stadelmann, P. A. Buffat, and J.-P. Borel, *Europhys. Lett.* 6, 349 (1988).
- 379. M. Flueli, R. Spycher, P. A. Stadelmann, P. A. Buffat, and J. P. Borel, IOP Publishing Ltd., Bristol (1988), p. 309.
- 380. D. A. Jefferson and A. I. Kirkland, in "Electron Beam Imaging of Non-Crystalline Materials" (K. Knowles, Ed.), p. 71. The Institute of Physics, Bristol, 1988.
- 381. M. Flueli, PhD Thesis, EPFL, Lausanne (1989).
- 382. P.-A. Buffat, M. Flüeli, R. Spycher, P. Stadelmann, and J.-P. Borel, *Faraday Discuss*. 92, 173 (1991).
- 383. W. Neumann and H. Hofmeister, in "Proc. Autumn School 1992 of the Int. Centre of Electron Microscopy" (J. Heydenreich and W. Neumann, Eds.), p. 183. MPI Halle, Halle, 1993.
- 384. J. Urban, Cryst. Res. Technol. 33, 1009 (1998).

- 385. D. K. Saha, K. Koga, and H. Takeo, Eur. Phys. J. D 9, 539 (1999).
- 386. J. A. Ascencio, M. Pérez, and M. J. Yacamán, Surf. Sci. 447, 73-80 (2000).
- 387. S. A. Nepijko, H. Hofmeister, H. Sack-Kongehl, and R. Schlögl, J. Cryst. Growth 213, 129 (2000).
- 388. J. Urban, H. Sack-Kongehl, K. Weiss, I. Lisiecki, and M.-P. Pileni, Cryst. Res. Technol. 35, 731 (2000).
- 389. J. A. Ascencio, M. Pérez-Alvarez, S. Tehuacanero, and M. José-Yacamán, Appl. Phys. A 73, 295 (2001).
- 390. H. Sauer and H. Sack-Kongehl, in "Abstracts Dreiländertagung Elektronenmikroskopie," p. 87. Innsbruck, 2001.
- 391. J. W. Kang and H. J. Hwang, Nanotechnology 13, 524 (2002).
- 392. I. Lisiecki, A. Filankembo, H. Sack-Kongehl, K. Weiss, M.-P. Pileni, and J. Urban, Phys. Rev. B 61, 4968 (2000).
- 393. A. Renou, J. M. Penisson, and M. F. Gillet, Z. Phys. D 12, 139 (1989).
- 394. W. Vogel, B. Rosner, and B. Tesche, J. Phys. Chem. B 97, 11611 (1993).
- 395. S. Ino, S. Ogawa, T. Taoka, and H. Akahori, Jpn. J. Appl. Phys. 11, 1859 (1972).
- 396. A. G. Dhere, R. J. de Angelis, P. J. Reucroft, and J. Bentley, Ultramicroscopy 18, 415 (1985).
- 397. W. Neumannn, J. Komrska, H. Hofmeister, and J. Heydenreich, Acta Crystallogr. A 4, 890 (1988).
- 398. C. Hintze, in "Handbuch der Mineralogie. I. Elemente und Sulfide," p. 236. Verlag von Veit und Co., Leipzig, 1904.
- 399. V. M. Kvasnytsya, Dokl. Acad. Nauk 7, 587 (1978).
- 400. C. H. Gammons, Can. Mineral. 34, 1 (1996).
- 401. G. Canizal, J. A. Ascencio, J. Gardea-Torresday, and M. J. Yacaman, J. Nanoparticle Res. 3, 475 (2001).
- 402. J. W. Kang and H. J. Hwang, J. Phys. C 14, 2629 (2002).
- 403. K. Hiraga, T. Oku, M. Hirabayashi, and T. Matsuda, J. Mater. Sci. Lett. 8, 130 (1989).
- 404. R. Hernandez, G. Diaz, A. Vazquez, Y. Reyesgasga, and M. J. Yacaman, Langmuir 7, 1546 (1991).
- 405. B. Pauwels, D. Bernaerts, S. Amelinckx, G. VanTendeloo, J. Joutsensaari, and E. I. Kauppinen, J. Cryst. Growth 200, 126 (1999).
- 406. A. E. Romanov, I. A. Polonsky, V. G. Gryaznov, S. A. Nepijko, T. Junghanns. and N. I. Vitrykhovski, J. Cryst. Growth 129, 691 (1993).
- 407. N. R. Avery and J. V. Sanders, J. Catal. 18, 129 (1970).
- 408. L. D. Marks and A. Howie, Nature 282, 196 (1979).
- 409. B. Moraweck and A. J. Renouprez, Surf. Sci. 106, 35 (1981).
- 410. M. J. Yacaman, S. Fuentes, and J. M. Domingues, Surf. Sci. 106, 472 (1981).
- 411. P. J. F. Harris, Int. Materials Review 40, 97 (1995).
- 412. M. J. Yacaman, M. Marin-Almazo, and J. A. Ascencio, J. Mol. Catal. A 173, 61 (2001).
- 413. H.-G. Boyen, G. Kästle, F. Weigl, B. Koslowski, C. Dietrich, P. Ziemann, J. P. Spatz, S. Riethmüller, C. Hartmann, M. Möller, G. Schmid, M. G. Garnier, and P. Oelhafen, Science 297, 1533 (2002).
- 414. S. T. Lee, N. Wang, Y. F. Zhang, and Y. H. Tang, MRS Bull. 24, 36 (1999).
- 415. J. Brandmüller and R. Claus, Indian J. Pure Appl. Phys. 26, 60 (1988).
- 416. J. Brandmüller and R. Claus, Croat. Chem. Acta 61, 267 (1988).
- 417. Y.-J. Jiang, L.-J. Liao, G. Chen, and P.-X. Zhang, Acta Crystallogr. A 46, 772 (1990).
- 418. F. Koberling, A. Mews, U. Kolb, I. Potapova, M. Burghard, and T. Basché, Appl. Phys. Lett. 81, 1116 (2002).
- 419. M. Gillet, Surf. Sci. 67, 139 (1977).
- 420. R. Monot, in "Proc. Int. Symp. on the Physics of Latent Image Formation in Silver Halides" (A. Baldereschi, Ed.), p. 175. World Scientific Publ., Singapore, 1984.
- 421. L. D. Marks, Rep. Prog. Phys. 57, 603 (1994).

- 422. M. J. Yacaman, J. A. Ascencio, H. B. Liu, and J. Gardea-Torresdey, J. Vac. Sci. Technol. B 19, 1091 (2001) nanian J. Mineral.
- 423. V. M. Kvasnytsya, Miner Zh 11 83 (1989) 78, 45 (1997) 424. G. Rose and A. Sadebeck, in "Physikalische Abhandlungen der Königlichen Akademie der Wissenschaften zu Berlin," p. 85. F. Dümmler's Verlagsbuchhandlung, Berlin, 1876.
- 425. P. Groth, in "Die Mineraliensammlung der Universität Strassburg. Ein Supplement zu den vorhandenen mineralogischen Handbüchern" (Karl J. Tübner, Ed.), p. 4. Strassbourg, 1878.
- 426. J. Kourimsky and F. Tvrz, in "Bunte Welt der Minerale," p. 59. Artia-Verlag, Prague, 1977.
- 427. J. Strüver, Atti della Reale Accademia dei Lincei 275, 109; plate 1 (1877).
- (1877). 'Ontogenesis of magnetite' 428. A. M. Dimkin and A. A. Permyakov, *Ural Naucn. Centr Akad.* Nauk USSR, Sverdlovsk (1984), p. 188.
- 429. G. Bögels, J. G. Buijnsters, S. A. C. Verhaegen, H. Meekes, P. Bennema, and D. Bollen, J. Cryst. Growth 203, 554 (1999).
- 430. O. Kitakami, H. Sato, Y. Shimada, F. Sato, and M. Tanaka, Phys. Rev. B 56, 13849 (1997).
- 431. M. Gillet and M. Brieu, Z. Phys. D 12, 107 (1989).
- 432. D.-L. Lu and K.-I. Tanaka, Surf. Sci. 409, 283 (1998).
- 433. M. J. Yacaman, M. Avalos-Borja, A. Vazquez, S. Tehuacanero, P. Schabes, and R. Herrera, in "Mat. Res. Symp. Proc." (R. D. Bringans, R. M. Feenstra, and J. M. Gibson, Eds.), p. 371. Materials Research Society, Pittsburgh, 1990.
- 434. Z. R. Dai, S. H. Sun, and Z. L. Wang, Surf. Sci. 505, 325 (2002).
- 435. G. Rupprechter, PhD Thesis, Leopold-Franzens-Universität Innsbruck (1995).
- 436. G. Rupprechter, K. Hayek, and H. Hofmeister, Nanostruct. Mater. 9, 311 (1997).
- 437. K. H. Kuo, in "Proc. XI. Int. Cong. on Electron Microscopy," The Japanese Society of Electron Microscopy, Tokyo, 1986, p. 159.
- 438. F. Robinson and M. Gillet, Thin Solid Films 98, 179 (1982).
- 439. A. Renou and J. M. Penisson, J. Cryst. Growth 78, 357 (1986).
- 440. S. Giorgio and J. Urban, Appl. Phys. Lett. 52, 1467 (1988).
- 441. G. Bögels, H. Meekes, P. Bennema, and D. Bollen, J. Phys. Chem. B 103, 7577 (1999).
- 442. M. Audier and P. Guyot, Acta Metall. Mater. 36, 1321 (1988).
- 443. K. S. Vecchio and .B. Williams D, Metall. Trans. A 19, 2875 (1988).
- 444. A. Rodriguez, C. Amiens, B. Chaudret, M.-J. Casanove, P. Lecante, and J. S. Bradley, Chem. Mater. 8, 1978 (1996).
- 445. A. Recnik and D. Kolar, in "Proceedings of the 11th European Conference on Electron Microscopy, Dublin 1996" (Committee of Europ. Soc. of Microsc., Ed.), p. 710. Brussels, 1998.
- 446. A. Recnik and D. Kolar, in "Proceedings of the 11th European Conference on Electron Microscopy, Dublin 1996" (Committee of Europ. Soc. of Microsc., Ed.), p. 712. Brussels, 1998.
- 447. C. Solliard, P. Buffat, and F. Faes, J. Cryst. Growth 32, 123 (1976).
- 448. J. G. Pérez-Ramírez, M. J. Yacamán, A. Díaz-Pérez, and L. R. Berriel-Valdos, Superlattices Microstruct. 1, 485 (1985).
- 449. A. R. Thölén, Phase Transitions 24-26, 375 (1990).
- 450. M. Shimoda, T. J. Sato, A. P. Tsai, and J. Q. Guo, Phys. Rev. B 62, 11288 (2000).
- 451. R. D. Field and H. L. Fraser, Mater. Sci. Eng. 68, L17 (1984–1985).
- 452. M. Arita, N. Suzuki, and I. Nishida, J. Cryst. Growth 132, 71 (1993).
- 453. H. Q. Ye, D. N. Wang, and K. H. Kuo, Ultramicroscopy 16, 273 (1985).
- 454. G. D. Sukhomlin and A. V. Andreeva, Phys. Status Solidi A 78, 333
- 455. D. Carron and R. Portier, in "Proc. 14th Int. Cong. Electron Microscopy" (H. A. Calderón Benavides and M. José Yacaman, Eds.), p. 13. IOP Publ., Bristol, 1998.
- 456. W. Luyten, G. van Tendeloo, S. Amelinckx, and J. L. Collins, Philos. Mag. A 66, 899 (1992).
- 457. M. Mikiyoshida, L. Rendon, S. Tehuacanero, M. J. Yacaman, Surf. Sci. 284, L444 (1993).